3-10-2018

Correlation of Solid Dosage Porosity and Tensile Strength with Acoustically Extracted Mechanical Properties

Xiaochi Xu
Clarkson University

Connor Mack
St. John Fisher College, cjm09075@students.sjfc.edu

Zachary J. Cleland
Consolidate Precision Products

Chaitanya Krishna Prasad Vallabh
Clarkson University

Vivek S. Dave
St. John Fisher College, vdave@sjfc.edu

Publication Information

Xu, Xiaochi; Mack, Connor; Cleland, Zachary J.; Vallabh, Chaitanya Krishna Prasad; Dave, Vivek S.; and Cetinkaya, Centin (2018). "Correlation of Solid Dosage Porosity and Tensile Strength with Acoustically Extracted Mechanical Properties." *International Journal of Pharmaceutics* 542.1-2, 153-163.

Correlation of Solid Dosage Porosity and Tensile Strength with Acoustically Extracted Mechanical Properties

Abstract

Currently, the compressed tablet and its oral administration is the most popular drug delivery modality in medicine. The accurate porosity and tensile strength characterization of a tablet design is vital for predicting its performance such as disintegration, dissolution, and drug-release efficiency upon administration as well as ensuring its mechanical integrity. In current work, a non-destructive contact ultrasonic approach and an associated testing procedure are presented and employed to quantify and relate the acoustically extracted mechanical properties of pharmaceutical compacts to direct porosity and tensile strength measurements. Based on a comprehensive set of experimental data, it is demonstrated how strongly the acoustic wave propagation is modulated and correlated to the tablet porosity and tensile strength of a compact made using spray-dried lactose and microcrystalline cellulose with varying mixture ratios. The effect of mixing ratio on the porosity and tensile strength on the resulting compacts is quantified and, with the acoustic experimental data, mixing ratio is related to the compact ultrasonic characteristics. The ultrasonic techniques provide a rapid, non-destructive means for evaluating compacts in formulation development and manufacturing. The presented approach and data could find critical applications in continuous tablet manufacturing, its real-time quality monitoring, as well as minimizing batch-to-batch quality variations.

Disciplines

Pharmacy and Pharmaceutical Sciences

Comments

This is the author's manuscript version of the article. The final published version is available through the publisher: https://doi.org/10.1016/j.ijpharm.2018.03.018

Authors

Xiaochi Xu, Connor Mack, Zachary J. Cleland, Chaitanya Krishna Prasad Vallabh, Vivek S. Dave, and Centin Cetinkaya

Prepared for Publication in *the International Journal of Pharmaceutics*

Correlation of Solid Dosage Porosity and Tensile Strength with Acoustically Extracted Mechanical Properties

Xiaochi Xu[1], Connor Mack[2], Zachary J. Cleland[3], Chaitanya Krishna Prasad Vallabh[1], Vivek S. Dave[2], and Cetin Cetinkaya[1]*

[1] Photo-Acoustics Research Laboratory
Department of Mechanical and Aeronautical Engineering
Clarkson University
Potsdam, NY 13699-5725, USA

[2]St. John Fisher College
Wegmans School of Pharmacy
Rochester, NY 14618, USA

[3]Consolidate Precision Products
Syracuse, NY 13037, USA

February 15, 2018

Version 01.21

**Corresponding author*

8 Clarkson Ave. CAMP 241 Box 5725

Potsdam, NY 13699-5725

E-mail: cetin@clarkson.edu Phone: (315) 268-6514 Fax: (315) 268 6695

Abstract

Currently, the compressed tablet and its oral administration is the most popular drug delivery modality in medicine. The accurate porosity and tensile strength characterization of a tablet design is vital for predicting its performance such as disintegration, dissolution, and drug-release efficiency upon administration as well as ensuring its mechanical integrity. In current work, a non-destructive contact ultrasonic approach and an associated testing procedure are presented and employed to quantify and relate the acoustically extracted mechanical properties of pharmaceutical compacts to direct porosity and tensile strength measurements. Based on a comprehensive set of experimental data, it is demonstrated how strongly the acoustic wave propagation is modulated and correlated to the tablet porosity and tensile strength of a compact made using spray-dried lactose and microcrystalline cellulose with varying mixture ratios. The effect of mixing ratio on the porosity and tensile strength on the resulting compacts is quantified and, with the acoustic experimental data, mixing ratio is related to the compact ultrasonic characteristics. The ultrasonic techniques provide a rapid, non-destructive means for evaluating compacts in formulation development and manufacturing. The presented approach and data could find critical applications in continuous tablet manufacturing, its real-time quality monitoring, as well as minimizing batch-to-batch quality variations.

Keywords: continuous manufacturing, real-time monitoring, solid dosage porosity, solid dosage tensile strength, acoustic characterization techniques, mechanical properties, physical properties

1. Introduction

The compressed tablet and its oral administration remain the most commonly used method of drug delivery in medicine today. It is well recognized that the performance of a dosage form is closely linked to the physical (mechanical) and chemical properties of all ingredients in the formulation and their processing parameters. A typical tablet can be constituted by excipients (up to 95% by weight of the formulation). The influence of raw material variability on the functionality of excipients during processing and manufacturing has been a subject of several recent studies due to its practical importance and reported cases (Dave et al., 2015; García-Muñoz, 2009; Koynov and Muzzio, 2016; Kushner IV, 2013). The production of pharmaceutical excipients uses a series of processing steps aimed at eliminating the natural variability of such materials. Despite such efforts, however, excipient variability is still not uncommon (Hancock and Garcia-Munoz, 2013).

Many regularly used excipients are available from several different manufacturers, and supply chain considerations make it necessary for a pharmaceutical product to have more than a single source for each raw material, bringing the consequence of variability between suppliers. Excipients are manufactured using batch processes, which may lead to the possibility of batch-to-batch variation in an excipient obtained even from the same manufacturer. A large number of pharmaceutical excipients are derived from natural products, making them susceptible to environmental changes (e.g., seasonal variations and transportation conditions) that affect the end characteristics of the raw materials (Chamarthy et al., 2009; Hancock and Garcia-Munoz, 2013; Landin et al., 1993; Maincent, 1999).

Bulk (apparent) mass density/porosity and tensile strength (yield strength/point) are important physical-mechanical properties of a tablet that are known to influence the disintegration,

dissolution, and drug-release efficiency upon administration. Routine evaluation of these properties during tablet manufacture is essential in ensuring consistency in tablet quality. Currently, these properties are mostly evaluated *offline*, following the guidelines provided by various pharmacopeias. Most of the pharmacopeial techniques are semi-destructive to the test samples. Moreover, some of these techniques may lack specificity and resolution. In the past two decades, an emphasis has been placed on continuous manufacturing and *online* (real-time) monitoring of the tablet properties and integrity. These past few years have also observed and a significant increase in the development of efficient, material-sparing, and non-destructive techniques for the evaluation of tablet properties (Fevotte et al., 2014). Such techniques include, near infrared spectroscopy (NIR), Raman spectroscopy, X-ray microtomography, nuclear magnetic resonance imaging (NMRI), terahertz pulsed imaging, laser-induced breakdown spectroscopy (LIBS), and thermal techniques. Each of these techniques is associated with its specific advantages and drawbacks (Dave et al., 2017).

Our laboratory has previously introduced and reported a set of a non-invasive, acoustics-based techniques for the characterization of tablet properties (I. Akseli et al., 2009; Ilgaz Akseli et al., 2009; Liu and Cetinkaya, 2010; Varghese and Cetinkaya, 2007; Smith et al., 2011; Vahdat et al., 2013)). The approach is based on the principle that the speeds of pressure and shear waves propagating in a medium depend on its elasticity (stiffness), and inertia (mass density) as well as its micro-granular structure. In typical solid dosage forms, “hardness”, porosity and mechanical strength (tensile strength) are closely correlated with its viscoelastic properties. Moreover, material texture (e.g., grain size and grain-to-grain mechanical coupling) and viscoelasticity affects the spectral dispersion of a composite compact material. Relating an experimentally acquired spectral dispersion relation to a visco-elastic material model with scattering effects, the

mechanical (e.g., elasticity, mass density, and viscoelasticity) and geometric (e.g., grain size distribution and inter-granular elastic stiffness) properties (Smith et al., 2011; Vahdat et al., 2013) can be extracted.

The dwell time of a typical commercial compaction press is on a millisecond scale ranging from ~5ms to over 80 ms while the acoustic pulse method of acquiring the Time-of-Flight (ToF) is on the microsecond (μs) scale (Akseli et al., 2008; Leskinen et al., 2010) thus allowing many acquisitions during a single compaction event (real-time *in-die* monitoring). It has been previously established that, by utilizing a non-destructive *off-line* acoustic pulse-echo method (Akseli and Cetinkaya, 2008; Liu et al., 2011; Liu and Cetinkaya, 2010; Smith et al., 2011), the mechanical properties of tablets with complex geometries such as dry-coated and layered tablets can be characterized. It was also shown that not only can in-die measurements be made, but they can be done wirelessly and also *in-line* (out-of-die post compaction), resulting in comparative differentiation in solid dosage mechanical properties (Stephens et al., 2013; Stephens et al., 2013; Stephens et al., 2012). Extracting material properties from the temporal, spectral and dispersive properties of propagating elastic (ultrasonic/acoustic) waves is a desirable approach due to its fast temporal responsiveness, non-destructive/non-invasive nature, potential in real-time in-die monitoring, as well as its relatively low equipment and operational cost. This initial research suggests that an in-die real-time monitoring system is plausible and within the capacity of current acoustic techniques and the availability of off-the-shelve hardware.

The issues with the quality and integrity of manufactured pharmaceutical products are a leading cause in the global drug supply shortages (accounting for 66% of shortages) (CDER, 2014). Proposed actions and remedies for these shortages are currently drafted by the Office of Pharmaceutical Quality (OPQ), formed in 2015, within the Food and Drug Administration's

(FDA) Center for Drug Evaluation and Research (CDER); with an emphasis on better process control and monitoring by improving monitoring metrics, techniques, fundamental process knowledge, and implementing modern quality control regiments (OPQ, 2015). These proposed rules and regulations could be viewed as a continuation of previous quality guidance efforts such as Scale-Up and Post-Approval Changes (SUPAC), Process Analytical Technology (PAT), and Quality by Design (QbD), which are adopted/co-developed by the European Medicines Agency (EMA) of the European Union (EU), and also observed by the Pharmaceuticals and Medical Devices Agency (PMDA) of Japan; continuing the same intent of reducing deficiency in pharmaceutical drug development and manufacture quality (Lawrence, 2008).

In current work, a non-destructive contact ultrasonic method was employed to quantify and correlate acoustically extracted mechanical properties in pharmaceutical compacts to direct measurements. This approach has some key practical applications in real-time process monitoring in tablet continuous manufacturing. Apart from the fact that the technique is sample-sparing, unlike other non-invasive techniques such as NIR, evaluation of tablet mechanical properties by ultrasonic method requires no calibration models development. The ultrasonic technique directly measures the physical (mechanical) properties of prepared compacts. Moreover, due to extremely rapid data acquisition durations (i.e. μs scale), the technique is amenable to continuous *online* real-time monitoring of tablet properties during tablet manufacture on a high-speed equipment. The current study is an attempt to establish a high degree of correlation between the tablet properties obtained from direct measurements and the acoustically extracted parameters.

2. MATERIALS AND METHODS

2.1 Preparation of Powder Mixes and Powder Materials

Spray-dried Lactose monohydrate, NF (Foremost™ Fast Flo® Lactose 316) was obtained from Kerry Inc. (Beloit, Wisconsin, USA). Microcrystalline Cellulose, NF, Ph. Eur., JP (Avicel® PH 102) was obtained from FMC BioPolymer (Newark, Delaware, USA). Binary mixes of microcrystalline cellulose (MCC) and lactose monohydrate (LAC) were prepared with the weight percentage ratios of 100:0, 75:25, 50:50, 25:75 and 0:100 (MCC:LAC). MCC and LAC were first de-clumped by independently passing through a sieve with mesh # 40. The powders were then charged in a twin-shell blender (V-blender, Patterson-Kelley Company, East Stroudsburg, Pennsylvania, USA) without the use of intensifier bar, and blended at 20 RPM (rotational per minute) for a period of five minutes. Magnesium Stearate was added as a lubricant to this blend after passing through a sieve with mesh # 40, and further blended for two minutes. After the completion of blending, the blended powders were double-bagged, sealed and stored at room temperature (23°C) for four weeks until utilized for the reported experiments.

2.2 Tablet Manufacturing

The tablets (compacts) of the blends were prepared on an instrumented, 10-station, single-layer, rotary tablet press (Piccola B-506, SMI Inc., Lebanon, New Jersey, USA) using 10 mm, flat-faced, "B" tooling (SMI Inc., Lebanon, New Jersey, USA). The target compact weight was set at 500 mg. The compacts were prepared at a constant tableting speed of 20 RPM. The compacts were prepared at six levels of compaction pressures (P_c), i.e. 12.74, 25.48, 50.96, 63.69, 76.43, and 89.17 MPa. The tableting speed and the compaction pressures were monitored live using the real-time display from the accompanying proprietary software (*the Director*, SMI Inc., Lebanon,

New Jersey, USA). The true densities of the samples (binary mixes) were measured using a helium displacement pycnometer (AccuPyc 1340, Micromeretics, Norcross, Georgia, USA) using the method specified in the USP (United States Pharmacopeia) 38 – NF 33, general chapter <699> on the density of solids. The true densities of neat materials as well as the binary mixes were measured in triplicate after the materials were equilibrated in a desiccator for at least 24 hours.

2.3 Tablet Sample Sets

In the reported experiments, five sample sets of cylindrical compacts (referred hereafter to as AL100-0, AL75-25, AL50-50, AL25-75, and AL0-100, respectively) made of MCC and LAC with the five (percentage) weight mixing ratios of 100:0, 75:25, 50:50, 25:75 and 0:100 were employed (Table 1). For each sample set, six data sets (for the compaction pressure levels of P_c = 12.74, 25.48, 50.96, 63.69, 76.43, and 89.17 MPa, respectively) are acquired and reported in Table 1. For each data set, 12 compacts were utilized. The total number of compacts in the study was 360. In Table 1, the tablet masses measured by a digital scale (A120S-L, Mettler-Toledo Inc., Columbus, Ohio, USA) with an error range of ± 50×10^{-6} g, geometric dimensions measured by digital calipers (CD-6 in CS Absolute Digimatic Caliper, Mitutoyo Inc., Aurora, Illinois, USA) with an error range of ± 5×10^{-6} m (Mitutoyo Model CD-6, Aurora, Illinois, USA) are reported.

2.4 Tablet Evaluation

The volume of a cylindrical tablet V with a radius of r and a thickness of h was calculated by $V = \pi r^2 h$. The mass porosity (ϕ^m) of the prepared tablets in percentage (%) was calculated using the bulk density of the compacts and true densities of the formulation and is defined by:

$$\phi^{m}(\%) = \left(1 - \frac{\rho_b}{\rho_t}\right) \times 100 \qquad 1$$

where ρ_b is the bulk density of the tablet and ρ_t is the true density of the porous material.

The weight variation of the prepared compacts was evaluated using the method specified in USP 38 – NF 33, general chapter <905> on the uniformity of dosage units. A set of tablets (n=12) were randomly selected from each batch, and individually weighed on an electronic balance, and the weight recorded.

The breaking force (diametrical crushing strength) of the prepared compacts was tested using the method specified in USP38 – NF33, *General Chapter Prospectus: Tablet Breaking Force <1217>*. Briefly, ten randomly selected tablets from each batch were tested using an automatic hardness tester (VK200, Varian, Inc., Cary, North Carolina, USA). The compact breaking force is recorded in kP (kiloponds) and further converted to tensile fracture strength (force/tablet cross-sectional area) in MPa units. In Table 2, the average tensile strengths σ_b^m and porosities ϕ^m of the tablets in the sample sets are reported.

2.5 Ultrasound Measurements

In the reported experiments, an ultrasonic experimental set-up based on an existing testing instrument (ATT2020, Pharmacoustics Technologies, LLC, Potsdam, New York, USA) was developed and employed. The ATT instrument is a computer-controlled ultrasonic waveform

acquisition and analysis system consisting of transducers, delay-lines, load monitoring system, a pulser/receiver board, and a tablet centering apparatus as well as a graphical user interface based on LabVIEW (LabVIEW 15, National Instruments Corp., Austin, Texas, USA) for convenient waveform acquisition and ToF analysis (Fig. 1.a). The ultrasonic instrument can operate both in pulse-echo (reflection) and pitch-catch (transmission) ultrasonic modes for pressure and shear waves (Krautkrämer and Krautkrämer, 2013). The reported experimental set-up (operating in pitch-catch mode) was utilized to acquire the ultrasonic responses for the characterization of the mechanical properties (both at macro and micro-scales) of the tablet materials.

In the reported experiments, the set-up consisted of two pressure transducers (AT024, Valpey Fisher, Hopkinton, Massachusetts, USA) with a central frequency of 2.25MHz, two shear transducers (E1574, Valpey Fisher, Hopkinton, Massachusetts, USA) with a central frequency of 1MHz, as well as the ATT ultrasonic instrument operated in pitch-catch mode. Both pressure and shear data were acquired for characterizing the mechanical properties of the tablets. In the reported pressure and shear experiments, the pulser/receiver parameters were set at a pulse width of 200ns, pulser voltage of 200V, a sampling rate of 100MHz (corresponding to a time resolution of 10ns), an amplification gain of 0dB, and an averaging (oversampling) rate of 512. In the pressure set-up (left apparatus in Fig. 1.a), Transducer 1 was coupled with the delay-line and screwed into the upper transducer holder. The function of the delay-line was to separate the initial ultrasonic pulse (main bang) generated by Transducer 1 from the interface reflections in the sample. Transducer 2 was directly screwed into the bottom transducer/sample holder. The transducer/sample holder apparatus was used to hold the sample while acquiring waveform and to allow two transducers move respect to each other. The tablet centering apparatus mounted on the transducer/sample holder was used to accurately/repeatably center and hold the tablets in

place while acquiring acoustic waveform data. The three-point structure-leveling platform was used to support the transducer/sample holder and calibrate the system. By parallelizing the holder platforms housing the transducers using adjustment knobs of the ATT2020 instrument, the contact between the transducer and tablet interface is maximized for acquiring high quality waveforms. The load cells are mounted at the bottom platform of the set up and a liquid crystal display (LCD) of the signal-conditioning unit was used to read and monitor the applied axial load during waveform acquisition. In experiments, the applied load was maintained at 1500±10g for ensuring repeatable transmission contact between the sample and the surfaces of the delay-line and transducer by flattening asperities which are approximated to be on the order of 10-100 μm from the particle size distribution in excipient powders. Compared to the compaction pressure levels (P_c = 12.74-89.17 MPa), the exerted axial force levels (on the order of few N) during acoustic experiments are low, thus no effect on microstructure of the sample interiors is anticipated. The applied load can be read, saved and displayed on the LCD and/or the LabVIEW graphical user interface of the ATT2020 instrument. In the shear set-up (right apparatus in Fig. 1.a), the apparatus with a pair of shear transducers have the same configurations as the pressure set-up. An ultrasonic shear gel (54-T04, Sonotech, Glenview, Illinois, USA) was used for increasing acoustic transmission between the sample and the surfaces of the delay-line and transducer in the shear test.

In both pressure and shear pitch-catch transmission experiments, a tablet was placed on the bottom sample/transducer holder such that the bottom surface of the sample contacted with the Transducer 2 properly. The parallelism of the transducer faces was verified with a light source (BRSLEDPEN-B, Rayovac, Madison, WI, USA). The tablet was centered and fixed by the tablet centering apparatus during experiments. Transducer 1 assembled with delay-line was vertically

placed in contact with the top surface of the tablet by manually lowering the upper transducer holder and exerting a constant axial force during measurements. An electrical pulse generated by the ultrasonic instrument first excites the top transducer, Transducer 1. The acoustic pulse transmitted through the delay-line and the sample placed on the bare surface of the bottom transducer, Transducer 2, is eventually received by the active element of Transducer 2. The received pulse containing the ToF information was acquired, digitized, signal-processed and saved as a digital waveform data file via the ATT2020 GUI interface.

3 RESULTS AND DISCUSSIONS

A set of pressure and shear waveforms acquired for a sample AL50-50 tablet at each compaction pressure (P_c) level are depicted in Fig. 1.b-c. In Fig. 1.b, the arrival of pressure waves shortens with P_c up to P_c = 50.96 MPa, which indicates that stiffness increase dominates mass density (inertia) increase due to compaction in this range of P_c. Above P_c = 50.96 MPa, stiffness increase and mass compaction are of similar order of magnitude as the wave arrival changes to less extent. In Fig. 1.c, a similar trend is observed for shear waves as well. The acquired pressure and shear waveforms are processed to obtain the pressure and shear ToF (Δt_L and Δt_T) determined by two time-frequency techniques, namely, the STFT (short-term Fourier Transform) or Gabor wavelet transform. A time-frequency technique is adopted when a wave propagation medium is dispersive, which requires the arrival time of wave energy at a particular frequency rather than wave amplitude of arriving waves (Drai et al., 2002). The ToF (Δt_L and Δt_T) in the sample set are the time interval from the time locations of the peaks of delay-line (t_{1peak}) and tablet (t_{2peak}), i.e., in Fig. 1.b, for Pressure_AL50-50_12.74 MPa to 89.17MPa, t_{1peak} = 2.34, 2.33, 2.34, 2.36, 2.35 and 2.36µsec, t_{2peak}.= 6.93, 4.94, 4.02, 3.61, 3.57 and 3.59µsec, and $\Delta t_L = t_{2peak} - t_{1peak}$ =

4.59, 2.61, 1.68, 1.25, 1.22 and 1.23 μsec, respectively, in Fig. 1.c, for Shear_AL50-50_12.74 MPa to 89.17 MPa, t_{1peak} = 13.18, 13.17, 13.18, 13.17, 13.18 and 13.17 μsec, t_{2peak} = 20.51, 16.86, 15.75, 15.10, 15.11 and 15.08 μsec, and $\Delta t_T = t_{2peak}.- t_{1peak}$ = 7.33, 3.69, 2.57, 1.93, 1.93 and 1.91 μsec, respectively. The corresponding average pressure (c_L) and shear (c_T) wave velocities in a tablet with a thickness of h are determined by

$$c_L = h / \Delta t_L \qquad c_T = h / \Delta t_T \tag{2}$$

where h is also the one-way wave travel distance in a tablet. The apparent Young's modulus is determined by $E_A = c_L^2 \times \rho_A$ where ρ_A is the apparent mass density of the samples. The Poisson's ratio is determined by

$$\nu = \frac{1}{2}\left(\frac{\kappa^2 - 2}{\kappa^2 - 1}\right) \tag{3}$$

where $\kappa = c_L / c_T$ is the ratio of pressure to shear wave speeds. The measured average sample tablet thickness (h) and diameter (d), mass (m) and apparent density (ρ_A), corresponding pressure and shear wave velocities (c_L and c_T), Poisson's ratio (ν) and apparent Young's modulus (E_A) are summarized in Table 1 and 3 for the sample set. The average tensile strengths σ_b^m and porosity ratios ϕ^m of the tablets in the sample sets in Table 2, are correlated to the acoustic data presented in Table 3.

From the acquired pressure and shear waveforms of the tablets (Fig. 1.b-c), the reflections (peak) of the tablet samples shift to the left with the increase in the compaction pressure (P_c) (implying a decrease in ToF). Note that this shifting trend is evident from P_c = 12.74 to 50.96 MPa, and decreased from P_c = 63.69 to 89.17 MPa, i.e. the pressure and shear ToF values decrease. The sample pressure wave ToF values for the tablet data set AL50-50 were obtained as Δt_L = 4.59, 2.61, 1.68, 1.25, 1.22 and 1.23 µsec for varying P_c level, respectively (Fig. 1.b-c). The shear wave ToF values were also determined as Δt_T = 7.33, 3.69, 2.57, 1.93, 1.93 and 1.91 µsec for each P_c, respectively. It clearly indicates the ToF is sensitive to the change in the compaction pressure (P_c).

From Tables 1 and 3, it was also observed that the apparent density (ρ_A), pressure (c_L) and shear (c_T) wave speeds and apparent Young's moduli (E_A) of the sample materials increase with the increasing compaction pressure (in the sample set AL50-50, c_L = 819.86, 1210.08, 1669.48, 2151.01, 2250.90 and 2278.63 m/sec, c_T = 507.82, 835.53, 1092.02, 1387.51, 1378.23 and 1402.95 m/sec, and E_A = 0.63, 1.78, 3.61, 6.34, 6.63 and 6.89 GPa, respectively).

Superimposed plots for c_L, c_T, E_A and v for each sample set as a function of the compaction pressure P_c are presented in Fig. 2. It is observed that the c_L, c_T, and E_A curves for AL100-0 are the highest and monotonically increased. However, with the introduction of LAC (spray-dried Lactose monohydrate) into the excipient mixtures (namely, AL75-25, AL50-50, AL25-75 and AL0-100), the c_L, c_T, and E_A curves exhibit points of inflexion around P_c = 50 MPa, indicating the increase in mass density dominates the increase in elastic and shear moduli after this level of P_c.

No particular trend was observed in the plot of ν (Fig.2.d). As evident from the slope of the ν-κ curve in Eq. 3, at low porosity levels, the sensitive of ν to $\kappa = c_L / c_T$ ratio increases and inaccuracy in the ToF measurements leads to substantial errors in determining low values of ν (usually below ν = 0.1). The accuracy of κ determination can be increased by using higher frequency transducers and advanced time-frequency signal processing techniques.

3.1 Mechanical Property Analysis of the Sample Compacts

The mechanical performance of the prepared compacts was analyzed using the commonly employed relationships, i.e. compressibility and tabletability. *Compressibility* is defined as the ability of a material to undergo a reduction in volume as a result of an applied pressure (Joiris et al., 1998; Sun and Grant, 2001). In other words, it is the extent to which a powder bed undergoes a volume reduction under axial pressure in a confined space. It is represented by a plot of the calculated compact porosity versus compression pressure (P_c/A_T) (A_T is the area of the tablet). *Tabletability* has been defined earlier as the capacity of a powdered material to be transformed into a tablet of given strength under the effect of compression pressure and is generally represented by a plot of compaction pressure (P_c) versus the tablet tensile strength (σ_b^m) (am Ende et al., 2007; Joiris et al., 1998; Sun and Grant, 2001). The compressibility profiles of pure Avicel® PH102 (MCC), pure lactose, and their binary mixtures of are shown in Fig. 3.a. In general, for both materials (MCC and LAC), the compact porosity decreased in a nonlinear manner with an increase in compaction pressure. Beyond P_c= 50.96 MPa, this decrease in porosity was less pronounced. While both materials showed volume reduction to a similar extent, a closer observation of the compressibility profiles shows, as expected, that pure lactose exhibited slightly better volume reduction than pure MCC. The binary mixtures exhibited compressibility profiles according to the weight ratio of the mixture components. The

viscoelastic properties of MCC and LAC are known to be different. Thus, these observations are consistent with the fact that lactose is known to deform *via* brittle fracture, whereas MCC is a plastically deforming material.

The tabletability profiles of pure MCC, pure lactose, and their binary mixtures are shown in Fig. 3.b. Similar to that observed with compressibility, both materials, i.e. MCC and LAC showed a nonlinear increase in the compact tensile strength σ_t^m with increasing compaction pressures P_c. Due to its plastically deforming behavior, MCC showed higher tabletability profile, i.e. compact tensile strength σ_t^m at a given compaction pressure P_c, compared to that of lactose. The binary mixes of both materials exhibited tabletability profiles in accordance with the weight ratio of the mixture components. These observations regarding the compressibility and tabletability of MCC and LAC are consistent with the findings reported earlier (Dave et al., 2013).

3.2 Correlation of the Tensile Strength σ_t^m with c_L, c_T, and E_A

In order to ascertain the reliability and predictability of ultrasonic technique in measuring the physical-mechanical properties of the prepared tablets, correlations between the measured properties prepared compacts and the acoustic parameters obtained from the temporal response waveform set for each sample were established. In Fig. 4.a, the correlations between the tensile strengths of tablets (σ_t^m) prepared from pure MCC, pure LAC and their binary mixes at various compaction pressures and the pressure velocity (c_L) are depicted. It is observed that for a given sample (binary mix), the pressure velocity c_L appeared to linearly increase with increasing the tablet tensile strengths. The calculated degree of correlation, i.e. R^2 was observed to be >95% for

all of the tested samples. Pure LAC (AL0-100) exhibited a significantly higher c_L values for a given tensile strength, compared to pure MCC (AL100-0). Moreover, c_L also appeared to be distinct and separated for each set of formulation (binary mix) and appeared to reflect the relative ratio of their composition (Fig.4.a).

In Fig. 4.b, the correlation values between the tensile strengths of tablets (σ_b^m) prepared from pure MCC (AL0-100), pure LAC (AL100-0) and their binary mixes at various compaction pressures and the shear velocity (c_T), digitally extracted from the waveform are included. Similar to the observations made with the pressure velocity (c_L), the shear velocity c_T was found to linearly increase with increasing the tablet tensile strength σ_b^m. For each set of samples, a high degree of correlation ($R^2 > 96\%$) was observed between the tensile strength σ_b^m of tablets and the extracted acoustic parameter c_T. As noted for c_L, the pure LAC samples (AL0-100) showed significantly higher values of c_T at a given tensile strength σ_b^m, compared to that observed with the pure MCC samples (AL100-0). Moreover, the c_T values of the binary mixes of LAC and MCC were found to be distinct and well-separated and reflected the relative ratio of their composition (Fig.4.b).

The established correlations between the tensile strengths of tablets (σ_b^m) prepared using pure LAC (AL0-100) and pure MCC (AL100-0), their binary mixes at various compaction pressures, and the apperant Young's modulus (E_A) calculated using the acoustically obtained parameters are shown in Fig. 4.c. The E_A values of the tested samples were found to linearly correlate with the measured tablet tensile strengths (σ_b^m). In general, the E_A values appeared to increase with increasing tensile strength. A high degree of correlation was observed between E_A and σ_b^m for the

tested samples, and calculated R^2 ranged between 96 and 99%. Moreover, pure LAC (AL0-100) exhibited a significantly higher E_A, compared to that of pure MCC (AL100-0). The E_A values for the binary mixes of MCC and LAC were observed to be between those of pure MCC (AL100-0) and pure LAC (AL0-100), and in accordance with the ratio of their composition (Fig.4.c).

In summary, the reported observations and results quantify the sensitivity and correlation of the extracted mechanical properties (c_L, c_T, and E_A) with the tensile strength (σ_b^m) of the compressed tablets, which is often utilized as a key, experimentally quantifiable physical property benchmark.

3.3 Correlation of Tablet Porosity ϕ^m with c_L, c_T, and E_A

Tablet porosity ϕ^m has been previously reported to correlate with tablet tensile strength σ_b^m (Dave et al. 2013). Thus, in addition to correlating the tensile strengths of the sample tablets with the acoustically derived parameters, we also attempted to directly correlate the approximated porosity of the tablets with the similar acoustic parameters, i.e. c_L, c_T, and E_A. Such direct correlations have practical consequences in tablet quality control and monitoring, as the technology to make acoustic measurements quickly is currently available.

The correlations between the measured porosities of tablets (ϕ^m) prepared from pure MCC (AL100-0), pure LAC (AL0-100) or their binary mixes at various compaction pressures (P_c) and the pressure velocity (c_L), digitally extracted from the waveform are depicted in Fig. 5.a. A linear correlation was established between the measured tablet porosity ϕ^m and c_L for each sample set of the reported study. The degree of correlation (R^2) between individual sample set ranged between 90 and 99%. Unlike the correlations observed between the tablet tensile strength (σ_b^m)

and c_L, however, the trend lines of c_L were not distinct or separated for the tablets prepared from neat materials or their binary mixes, namely it is found that the pressure velocity (c_L) at a given tablet porosity (ϕ^m) appeared to overlap between different sample sets, particularly for tablets at ϕ^m between 15 and 25% (Fig.5.a).

In Fig. 5.b, the correlations between the measured porosities of tablets (ϕ^m) prepared from pure MCC (AL100-0), pure LAC (AL0-100) or their binary mixes at various compaction pressures (P_c) and the shear velocity (c_T), digitally extracted from the waveform are included. Similar to the observations with pressure velocity (c_L), for the reported sample sets (AL100-0, AL75-25, AL50-50, AL25-75 and AL0-100), the shear velocity (c_T) was found to linearly decrease with decreasing tablet porosity ϕ^m. For each set of samples, a high degree of correlation ($R^2 > 95\%$) was observed between porosity levels ϕ^m of tablets and the extracted acoustic parameter c_T. Moreover, similar to the observations above (Fig.5.a), the shear velocity (c_T) at a given porosity appeared to overlap between different sample sets (AL100-0, AL75-25, AL50-50 and AL25-75), particularly, for tablets at porosities between 15 and 25%. The trend lines of c_T for tablets prepared from neat materials or their binary mixes were not found to be distinct or separated.

The correlations between the porosities of tablets (ϕ^m) prepared using pure MCC (AL100-0), pure LAC (AL0-100), or their binary mixes at various compaction pressures (P_c), and the Young's modulus (E_A) calculated using the acoustically obtained parameters are shown in Fig. 5.c. An exponential correlation was established between the measured tablet porosity ϕ^m and E_A for each sample set of the reported study. As expected, the estimated E_A values of the tested samples were found to linearly correlate with the measured tablet porosities (ϕ^m). In general, the E_A values (Table. 3) appeared to decrease with decreasing tensile strength. A high degree of correlation was observed between E_A and porosity ϕ^m for the tested samples (Fig.5.c) and

calculated R^2 ranged between 96 and 99%. The trend lines of E_A for tablets with different composition were found to overlap for tablets at porosities between 15 and 25%.

CONCLUSIONS AND REMARKS

An acoustic ultrasound experimental approach is employed and reported to evaluate the relationship between the ultrasonic responses of pharmaceutical solid dosages to the two key manufacturing parameters, mixing ratios (MCC:LAC) in the range of 100:0 – 0:100 and compaction pressures P_c, in the range of 12.74 – 89.17 MPa). The analysis of experimental data correlating the acoustic experimental (pressure velocity (c_L), shear velocity (c_T) and apparent Young's modulus (E_A)) and resulting physical properties (compact porosity (ϕ^m) and tensile strengths (σ_b^m)) are also reported. The reported approach can be employed to determine both porosity and the tensile strength of the tablet from acoustic measurements in a non-destructive, rapid manner.

Based on the Time-of-Flight (ToF) (Δt_L and Δt_T) results of pressure (longitudinal) and shear (transverse) wave propagation in the tablet data sets, the apparent Young's modulus (E_A) and Poisson's ratios (ν) of the tablet materials were extracted and reported. It was noted that the apparent Young's moduli (E_A) of the samples (for varying mixing ratios (MCC:LAC) in the range of 100:0 - 0:100) increase with the increase in the compaction pressure P_c, and plateau after a critical compaction pressure level, concluding that the mechanical properties (c_L, c_T and E_A) of the tablets correlate with the compaction pressure (P_c). Experimentally obtained c_L, c_T and

extracted E_A for each compaction pressure level decrease with the decreasing material ratio of Avicel (MCC) from 100% to 25% (from AL100-0 to AL25-75).

In all the reported data sets (AL100-0 to AL25-75), E_A and porosity ratio (ϕ^m) are inversely correlated, whereas E_A and tensile strength (σ_b^m) are linearly (directly) correlated. It was found that Poisson's ratio (v) was not in correlation with porosity ratio ϕ^m or tensile strength σ_b^m due to the inaccuracies associated with the measurement precision of pressure and shear wave speeds using the energy methods (STFT and Wavelet transforms).

The current study presents a non-invasive, practical, and easy-to-use approach for characterizing the physical-mechanical properties of pharmaceutical tablets. This time- and material-sparing approach can have potential applications at various stages of tablet product development and research. For example, during pre-formulation and formulation stages, the physical-mechanical characterization of neat materials, as well as complex formulations, is a critical step. Using acoustic technique as a non-invasive approach for characterization can assist in optimizing the formulation and process variables with minimal material loss. During manufacturing, this technique can further minimize the time required for product quality checks. Additionally, the technique is amenable to in-line analysis of product quality, further saving time and material during manufacturing and process optimization. In sum, this approach potentially complements the USFDA's QbD-PAT paradigm recommended for tablet product development and approval.

ACKNOWLEDGEMENTS

Authors acknowledge funding from the Wallace H. Coulter Foundation for the acquisition of the experimental set-up utilized in the reported work and student support, and Pharmacoustics Technologies, LLC for technical support with the ATT2020 instrument.

LIST OF REFERENCES

Akseli, I., Becker, D.C., Cetinkaya, C., 2009. Ultrasonic determination of Young's moduli of the coat and core materials of a drug tablet. Int. J. Pharm. 370, 17–25.

Akseli, I., Cetinkaya, C., 2008. Acoustic testing and characterization techniques for pharmaceutical solid dosage forms. J. Pharm. Innov. 3, 216–226.

Akseli, I., Hancock, B.C., Cetinkaya, C., 2009. Non-destructive determination of anisotropic mechanical properties of pharmaceutical solid dosage forms. Int. J. Pharm. 377, 35–44.

Akseli, I., Libordi, C., Cetinkaya, C., 2008. Real-time acoustic elastic property monitoring of compacts during compaction. J. Pharm. Innov. 3, 134–140.

am Ende, M.T., Moses, S.K., Carella, A.J., Gadkari, R.A., Graul, T.W., Otano, A.L., Timpano, R.J., 2007. Improving the content uniformity of a low-dose tablet formulation through roller compaction optimization. Pharm. Dev. Technol. 12, 391–404.

CDER, 2014. Report to Congress: Second Annual Report on Drug Shortages for Calendar Year 2014, in: Administration, D.o.H.a.H.S.F.a.D. (Ed.).

Chamarthy, S.P., Pinal, R., Carvajal, M.T., 2009. Elucidating raw material variability—importance of surface properties and functionality in pharmaceutical powders. AAPS PharmSciTech 10, 780.

Dave, V.S., Fahmy, R.M., Hoag, S.W., 2013. Investigation of the physical–mechanical properties of Eudragit® RS PO/RL PO and their mixtures with common pharmaceutical excipients. Drug Dev. Ind. Pharm. 39, 1113–1125.

Dave, V.S., Saoji, S.D., Raut, N.A., Haware, R.V., 2015. Excipient variability and its impact on dosage form functionality. J. Pharm. Sci. 104, 906–915.

Dave, V.S., Shahin, H.I., Youngren-Ortiz, S.R., Chougule, M.B., Haware, R.V., 2017. Emerging technologies for the non-invasive characterization of physical-mechanical properties of tablets. Int. J. Pharm.

Drai, R., Khelil, M., Benchaala, A., 2002. Time frequency and wavelet transform applied to selected problems in ultrasonics NDE. NDT E Int. 35, 567–572. https://doi.org/10.1016/S0963-8695(02)00041-5

Fevotte, G., Wang, X., Ouabbas, Y., 2014. Acoustic Emission, a New Sensor for Monitoring Industrial Crystallization Processes. IFAC Proc. Vol. 47, 2727–2733.

García-Muñoz, S., 2009. Establishing multivariate specifications for incoming materials using data from multiple scales. Chemom. Intell. Lab. Syst. 98, 51–57.

Hancock, B.C., Garcia-Munoz, S., 2013. How do formulation and process parameters impact blend and unit dose uniformity? Further analysis of the product quality research institute blend uniformity working group industry survey. J. Pharm. Sci. 102, 982–986.

Joiris, E., Di Martino, P., Berneron, C., Guyot-Hermann, A.-M., Guyot, J.-C., 1998. Compression behavior of orthorhombic paracetamol. Pharm. Res. 15, 1122–1130.

Koynov, S., Muzzio, F.J., 2016. A quantitative approach to understand raw material variability. Process Simul. Data Model. Solid Oral Drug Dev. Manuf. 85–104.

Krautkrämer, J., Krautkrämer, H., 2013. Ultrasonic testing of materials. Springer Science & Business Media.

Kushner IV, J., 2013. Utilizing quantitative certificate of analysis data to assess the amount of excipient lot-to-lot variability sampled during drug product development. Pharm. Dev. Technol. 18, 333–342.

Landin, M., Martinez-Pacheco, R., Gomez-Amoza, J.L., Souto, C., Concheiro, A., Rowe, R.C., 1993. Effect of country of origin on the properties of microcrystalline cellulose. Int. J. Pharm. 91, 123–131.

Lawrence, X.Y., 2008. Pharmaceutical quality by design: product and process development, understanding, and control. Pharm. Res. 25, 781–791.

Leskinen, J.T., Simonaho, S.-P., Hakulinen, M., Ketolainen, J., 2010. In-line ultrasound measurement system for detecting tablet integrity. Int. J. Pharm. 400, 104–113.

Liu, J., Cetinkaya, C., 2010. Mechanical and geometric property characterization of dry-coated tablets with contact ultrasonic techniques. Int. J. Pharm. 392, 148–155.

Liu, J., Stephens, J.D., Kowalczyk, B.R., Cetinkaya, C., 2011. Real-time in-die compaction monitoring of dry-coated tablets. Int. J. Pharm. 414, 171–178.

Maincent, P., 1999. EXCIPIENTS-Potential problems when switching from one excipient to another one in drug formulation. Therapie 54, 5–10.

OPQ, 2015. Request for Quality Metrics Guidance for Industry, in: USDHH, F., CDER, CBER, OPQ (Ed.).

Smith, C.J., Stephens, J.D., Hancock, B.C., Vahdat, A.S., Cetinkaya, C., 2011. Acoustic assessment of mean grain size in pharmaceutical compacts. Int. J. Pharm. 419, 137–146.

Stephens, J.D., Kowalczyk, B.R., Hancock, B.C., Kaul, G., Akseli, I., Cetinkaya, C., 2012. In-die ultrasonic and off-line air-coupled monitoring and characterization techniques for drug tablets, in: AIP Conference Proceedings. AIP, pp. 1691–1698.

Stephens, J.D., Kowalczyk, B.R., Hancock, B.C., Kaul, G., Cetinkaya, C., 2013. Ultrasonic real-time in-die monitoring of the tablet compaction process—A proof of concept study. Int. J. Pharm. 442, 20–26.

Stephens, J.D., Lakshmaiah, M.V., Kowalczyk, B.R., Hancock, B.C., Cetinkaya, C., 2013. Wireless transmission of ultrasonic waveforms for monitoring drug tablet properties and defects. Int. J. Pharm. 442, 35–41.

Sun, C., Grant, D.J., 2001. Influence of crystal structure on the tableting properties of sulfamerazine polymorphs. Pharm. Res. 18, 274–280.

Vahdat, A.S., Vallabh, C.K.P., Hancock, B.C., Cetinkaya, C., 2013. Ultrasonic approach for viscoelastic and microstructure characterization of granular pharmaceutical tablets. Int. J. Pharm. 454, 333–343.

Varghese, I., Cetinkaya, C., 2007. Noncontact photo-acoustic defect detection in drug tablets. J. Pharm. Sci. 96, 2125–2133.

Table 1. Mixture ratio (%) and compaction pressure P_c levels (in the range of 12.74-89.17 MPa) of powders used in the five sample sets of cylindrical tablets (i.e. AL100-0, AL75-25, AL50-50, AL25-75, and AL0-100), and their average measured tablet thicknesses (h) and diameters (d), masses (m) and apparent mass densities (ρ_A) with corresponding standard deviations.

	Components								
	MCC	**LAC**	**Measured Parameter**	**P_c (MPa)**					
Sample Set	**Mixture Ratio (%)**			**12.74**	**25.48**	**50.96**	**63.69**	**76.43**	**89.17**
AL100-0	100	0	h (mm)	3.653±0.011	3.061±0.017	2.783±0.015	2.746±0.016	2.688±0.018	2.683±0.019
			d (mm)	10.039±0.003	10.012±0.004	9.993±0.005	9.992±0.006	9.992±0.006	9.988±0.005
			m (g)	0.298±0.001	0.299±0.001	0.300±0.001	0.306±0.001	0.304±0.001	0.303±0.001
			ρ_A (kg/m³)	1031.42±6.42	1240.68±8.15	1375.47±5.12	1419.14±9.59	1443.69±8.18	1444.49±11.70
AL75-25	75	25	h (mm)	3.681±0.008	3.144±0.009	2.798±0.063	2.715±0.012	2.652±0.017	2.633±0.012
			d (mm)	10.068±0.004	10.044±0.005	10.012±0.013	10.003±0.008	9.995±0.007	9.996±0.005
			m (g)	0.303±0.001	0.305±0.001	0.306±0.001	0.306±0.002	0.303±0.001	0.306±0.008
			ρ_A (kg/m³)	1033.58±4.16	1223.45±5.70	1374.48±3.13	1436.79±9.66	1458.79±9.15	1481.73±3.98
AL50-50	50	50	h (mm)	3.693±0.015	3.113±0.008	2.823±0.012	2.665±0.017	2.654±0.015	2.638±0.012
			d (mm)	10.088±0.004	10.068±0.004	10.062±0.004	10.013±0.005	10.018±0.005	10.017±0.007
			m (g)	0.303±0.001	0.303±0.001	0.303±0.001	0.302±0.001	0.305±0.001	0.305±0.001
			ρ_A (kg/m³)	1027.91±4.95	1221.76±4.59	1349.87±3.65	1440.19±8.66	1457.92±6.52	1469.58±8.67
AL25-75	25	75	h (mm)	3.551±0.010	3.087±0.027	2.796±0.012	2.670±0.013	2.655±0.018	2.616±0.012
			d (mm)	10.096±0.005	10.082±0.004	10.050±0.001	10.011±0.012	10.013±0.005	10.014±0.007
			m (g)	0.301±0.001	0.301±0.002	0.305±0.002	0.305±0.001	0.305±0.001	0.304±0.001
			ρ_A (kg/m³)	1058.47±4.92	1222.07±7.92	1375.90±5.07	1450.19±7.10	1460.97±9.09	1478.25±7.29
AL0-100	0	100	h (mm)	3.404±0.017	3.058±0.009	2.779±0.008	2.693±0.012	2.665±0.014	2.638±0.012
			d (mm)	10.051±0.010	10.056±0.012	10.057±0.012	10.030±0.004	10.030±0.006	10.033±0.006
			m (g)	0.304±0.001	0.304±0.002	0.302±0.001	0.303±0.001	0.305±0.001	0.305±0.001
			ρ_A (kg/m³)	1126.09±6.40	1251.07±5.79	1370.19±3.27	1425.07±6.19	1450.17±9.87	1463.08±7.94

Table 2. The average value of the tablet porosity (ϕ^m) and tensile strength (σ_b^m) with standard deviations in the five sample sets obtained from the *direct* measurement for compaction pressure (P_c).

Sample Set	Measured Parameters	P_c (MPa)					
		12.74	**25.48**	**50.96**	**63.69**	**76.43**	**89.17**
AL100-0	ϕ^m(%)	33.10 ± 0.61	20.08 ± 0.51	11.31 ± 0.44	10.42 ± 0.45	9.72 ± 0.45	9.44 ± 0.48
	σ_b^m (kPa)	11.40 ± 0.58	21.56 ± 0.63	31.03 ± 1.36	30.18 ± 1.00	30.60 ± 0.93	30.85 ± 0.74
AL75-25	ϕ^m(%)	32.88 ± 0.44	21.07 ± 0.29	11.17 ± 1.15	9.74 ± 0.51	8.50 ± 0.47	8.37 ± 0.66
	σ_b^m (kPa)	6.77 ± 0.29	13.67 ± 0.57	23.44 ± 0.73	29.44 ± 0.89	30.18 ± 0.85	30.78 ± 1.12
AL50-50	ϕ^m(%)	32.01 ± 0.81	20.20 ± 0.40	11.38 ± 0.59	8.86 ± 0.72	8.08 ± 0.87	7.55 ± 0.92
	σ_b^m (kPa)	3.54 ± 0.23	9.27 ± 0.34	17.23 ± 0.45	22.78 ± 0.44	24.69 ± 0.69	25.53 ± 0.72
AL25-75	ϕ^m(%)	30.50 ± 0.58	20.94 ± 0.63	12.44 ± 0.48	9.35 ± 0.01	8.10 ± 0.51	6.79 ± 0.69
	σ_b^m (kPa)	1.63 ± 0.08	4.65 ± 0.33	10.51 ± 0.30	18.41 ± 0.63	19.53 ± 0.46	20.92 ± 0.67
AL0-100	ϕ^m(%)	26.44 ± 0.61	18.51 ± 0.38	11.79 ± 0.44	7.55 ± 0.74	6.27 ± 0.45	5.14 ± 0.59
	σ_b^m (kPa)	3.34 ± 0.08	6.36 ± 0.31	10.57 ± 0.09	15.25 ± 0.76	18.04 ± 1.19	19.57 ± 0.85

Table 3. The average apparent Young's moduli (E_A), Poisson's ratio (v), pressure (c_L) and shear (c_T) wave speeds with their standard deviations for the five sample sets obtained from the acoustic tablet testing set-up.

Sample Set	Extracted Parameters	P_c (MPa)					
		12.74	**25.48**	**50.96**	**63.69**	**76.43**	**89.17**
AL100-0	E_A (GPa)	1.27 ± 0.03	2.48 ± 0.07	3.57 ± 0.06	3.92 ± 0.09	4.03 ± 0.13	4.02 ± 0.08
	v	0.025 ± 0.021	0.033 ± 0.017	0.029 ± 0.017	0.088 ± 0.033	0.077 ± 0.040	0.053 ± 0.023
	c_L (m/sec)	1111.44 ± 12.97	1414.61 ± 21.92	1612.06 ± 14.66	1678.13 ± 27.95	1684.83± 39.26	1675.04 ± 21.10
	c_T (m/sec)	775.51 ± 5.25	982.71 ± 10.82	1122.75 ± 9.62	1126.22 ± 12.02	1138.65 ± 21.74	1150.09 ± 9.39
AL 75-25	E_A (GPa)	0.83 ± 0.01	2.07 ± 0.04	3.67 ± 0.12	5.28 ± 0.16	5.47 ± 0.09	5.44 ± 0.23
	v	0.023 ± 0.017	0.026 ± 0.022	0.073 ± 0.034	0.097 ± 0.022	0.157 ± 0.013	0.124 ± 0.032
	c_L (m/sec)	899.08 ± 6.68	1301.63 ± 14.67	1645.79 ± 49.03	1938.86 ± 39.12	1996.38 ± 19.08	1954.03 ± 48.12
	c_T (m/sec)	628.24 ± 4.29	907.54 ± 11.53	1115.63 ± 23.66	1294.02 ± 14.68	1273.42 ± 13.16	1277.86 ± 10.57
AL 50-50	E_A (GPa)	0.63 ± 0.02	1.78 ± 0.06	3.61 ± 0.13	6.34 ± 0.11	6.63 ± 0.17	6.89 ± 0.22
	v	0.187 ± 0.026	0.041 ± 0.042	0.124 ± 0.036	0.143 ± 0.021	0.198 ± 0.024	0.191 ± 0.039
	c_L (m/sec)	819.86 ± 16.46	1210.08 ± 27.18	1669.48 ± 43.61	2151.01 ± 32.97	2250.90 ± 64.66	2278.63 ± 81.72
	c_T (m/sec)	507.82 ± 6.65	835.53 ± 17.28	1092.02 ± 13.88	1387.51 ± 10.83	1378.23 ± 10.79	1402.95 ± 18.79
AL 25-75	E_A (GPa)	0.57 ±0.03	1.54 ± 0.06	3.47 ± 0.18	6.80 ± 0.31	7.65 ± 0.31	8.18 ± 0.34
	v	0.240 ± 0.047	0.101 ± 0.069	0.040 ± 0.033	0.132 ± 0.047	0.136 ± 0.042	0.195 ± 0.047
	c_L (m/sec)	800.18 ± 29.28	1141.79 ± 28.60	1593.28 ± 43.57	2219.17 ± 93.96	2347.46 ± 91.01	2486.66 ± 119.95
	c_T (m/sec)	465.20 ± 19.27	757.10 ± 19.82	1101.38 ± 19.97	1439.44 ± 12.95	1518.70 ± 14.81	1521.71 ± 13.68
AL 0-100	E_A (GPa)	2.01 ± 0.04	3.59 ± 0.08	6.27 ± 0.18	7.70 ± 0.34	9.30 ± 0.34	9.46 ± 0.42
	v	0.180 ± 0.026	0.193 ± 0.025	0.216 ± 0.024	0.182 ± 0.049	0.207 ± 0.047	0.203 ± 0.048
	c_L (m/sec)	1393.11 ± 21.92	1780.88 ± 35.67	2284.42 ± 66.88	2436.83 ± 100.76	2700.86 ± 143.76	2703.62 ± 145.71
	c_T (m/sec)	869.15 ± 14.50	1096.66 ± 12.40	1372.04 ± 16.90	1512.31 ± 26.11	1630.28 ± 26.47	1639.62 ± 10.99

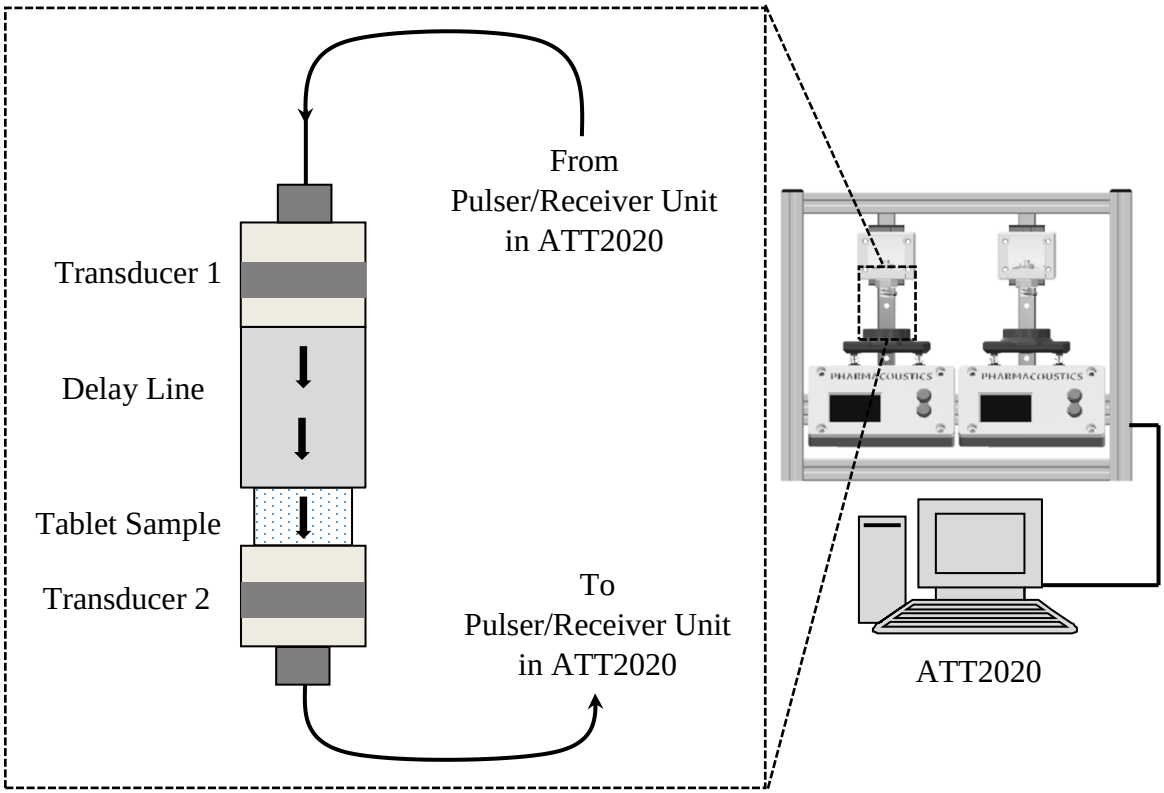
From
Pulser/Receiver Unit
in ATT2020
Transducer 1
Delay Line
Tablet Sample
Transducer 2
To
Pulser/Receiver Unit
in ATT2020
PHARMACOUSTICS
PHARMACOUSTICS
ATT2020

Figure 1.a

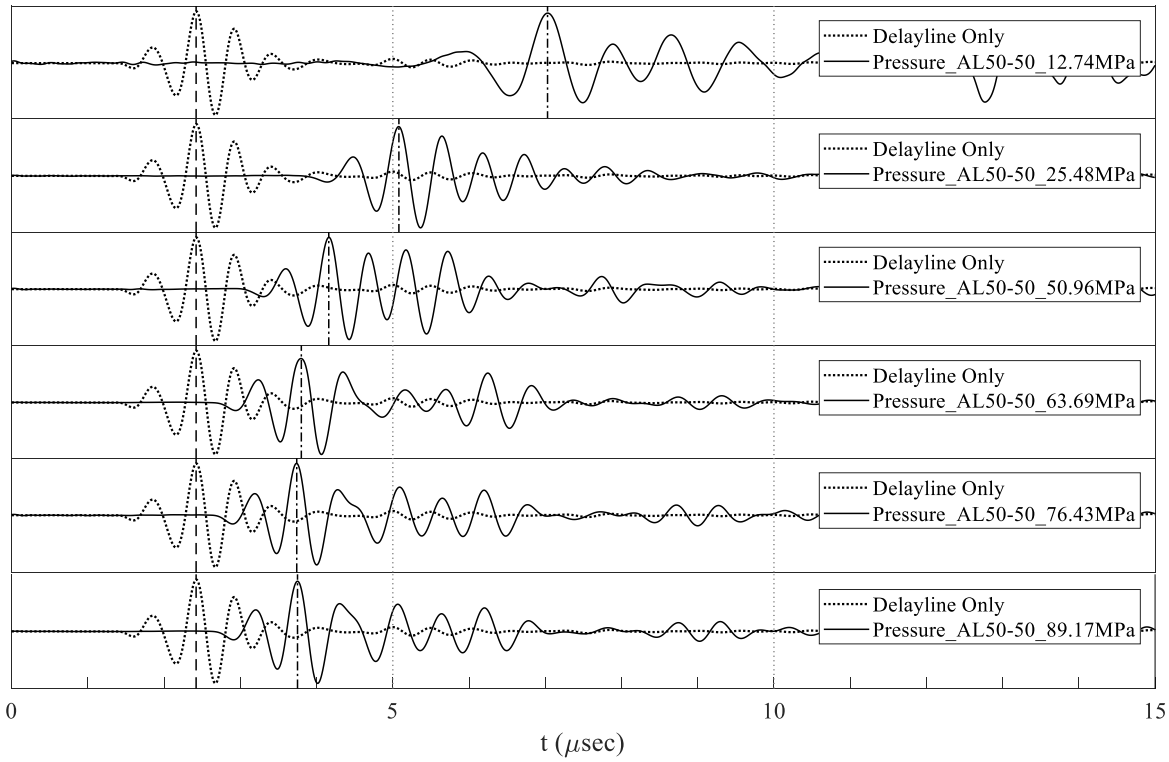
Delayline Only
Pressure_AL50-50_12.74MPa
Delayline Only
Pressure_AL50-50_25.48MPa
Delayline Only
Pressure_AL50-50_50.96MPa
Delayline Only
Pressure_AL50-50_63.69MPa
Delayline Only
Pressure_AL50-50_76.43MPa
Delayline Only
Pressure_AL50-50_89.17MPa
0
5
10
15
t (μsec)

Figure 1.b

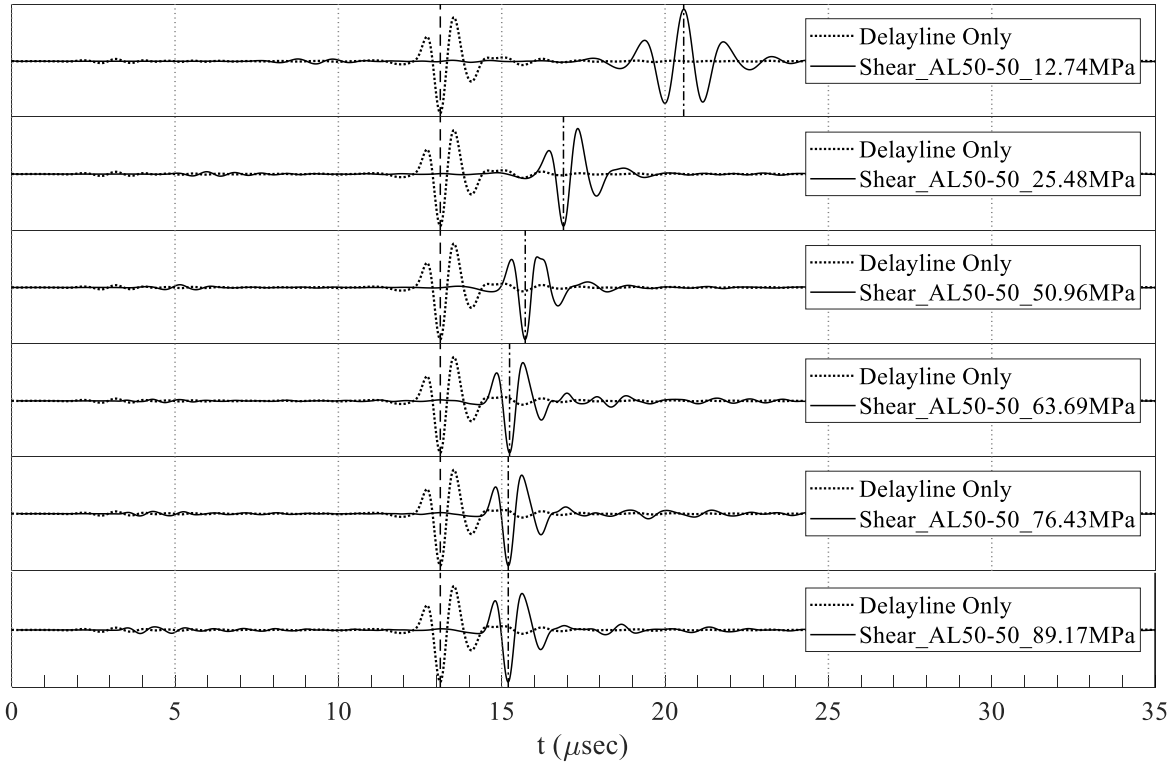

Figure 1.c

Figure 1. (*a*) Instrumentation diagram of the experimental set-up operating in the pitch-catch mode. Normalized pressure (*b*) and shear (*c*) waveforms for a tablet from the sample set AL50-50 with the corresponding compaction pressure levels indicated in insets. The effect of compaction pressure P_c on the propagation speeds c_L and c_T is clearly visible, as the wave arrival times (i.e. ToF) decrease with the increasing P_c in the sample set.

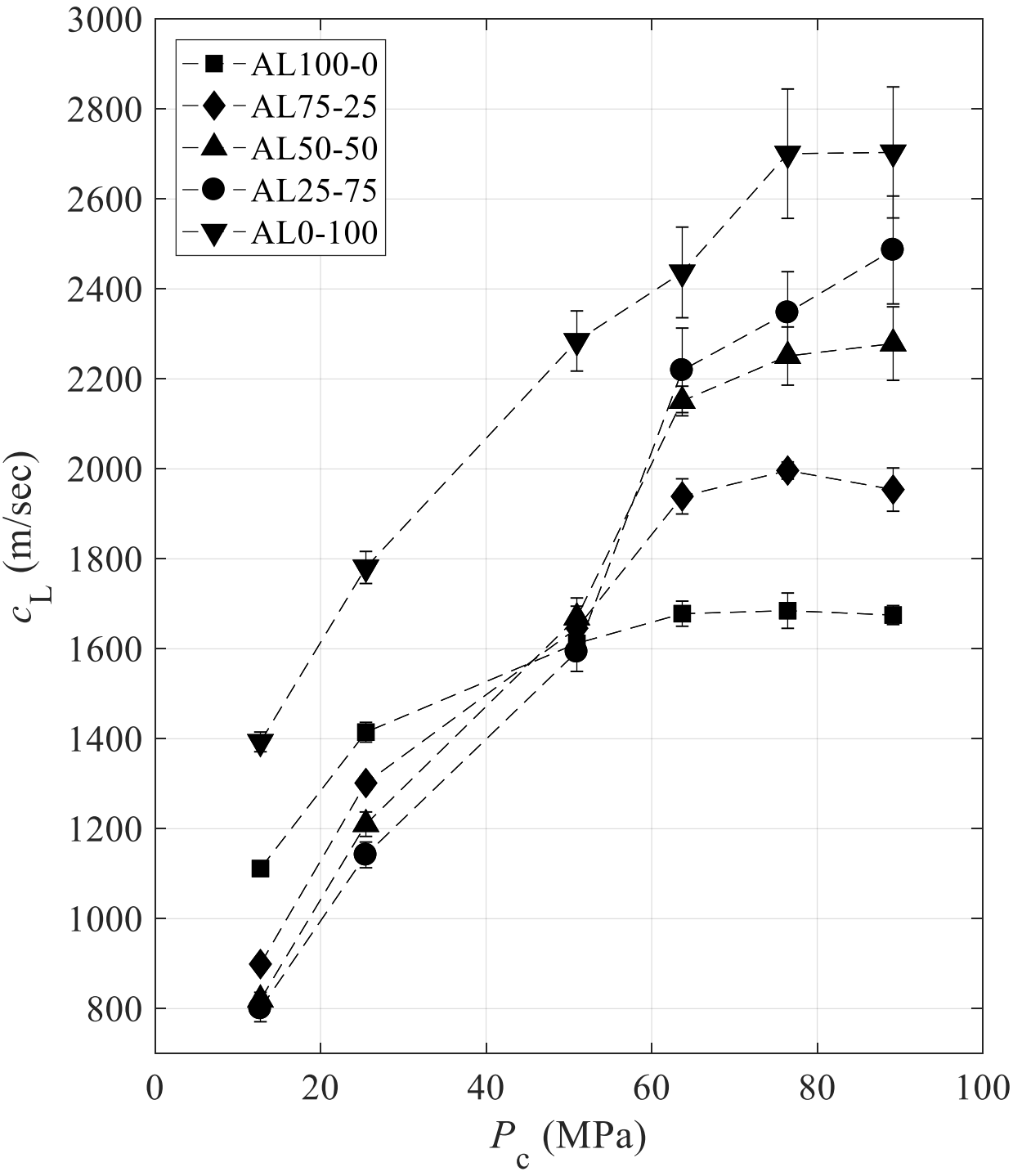
AL100-0
AL75-25
AL50-50
AL25-75
AL0-100
3000
2800
2600
2400
2200
2000
1800
1600
1400
1200
1000
800
c_L (m/sec)
0
20
40
60
80
100
P_c (MPa)

Figure 2.a

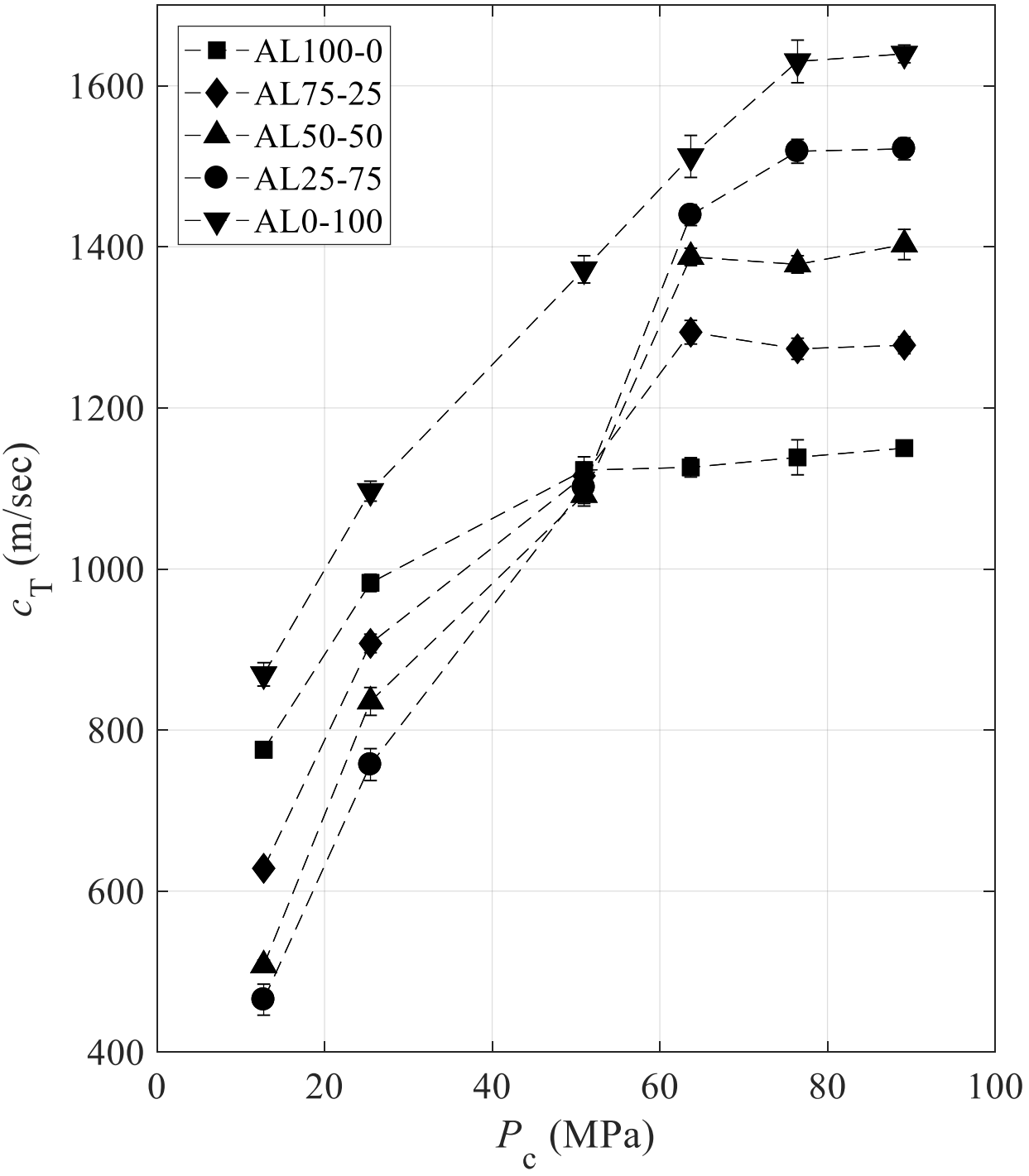
AL100-0
AL75-25
AL50-50
AL25-75
AL0-100
1600
1400
1200
1000
800
600
400
0
20
40
60
80
100
c_T (m/sec)
P_c (MPa)

Figure 2.b

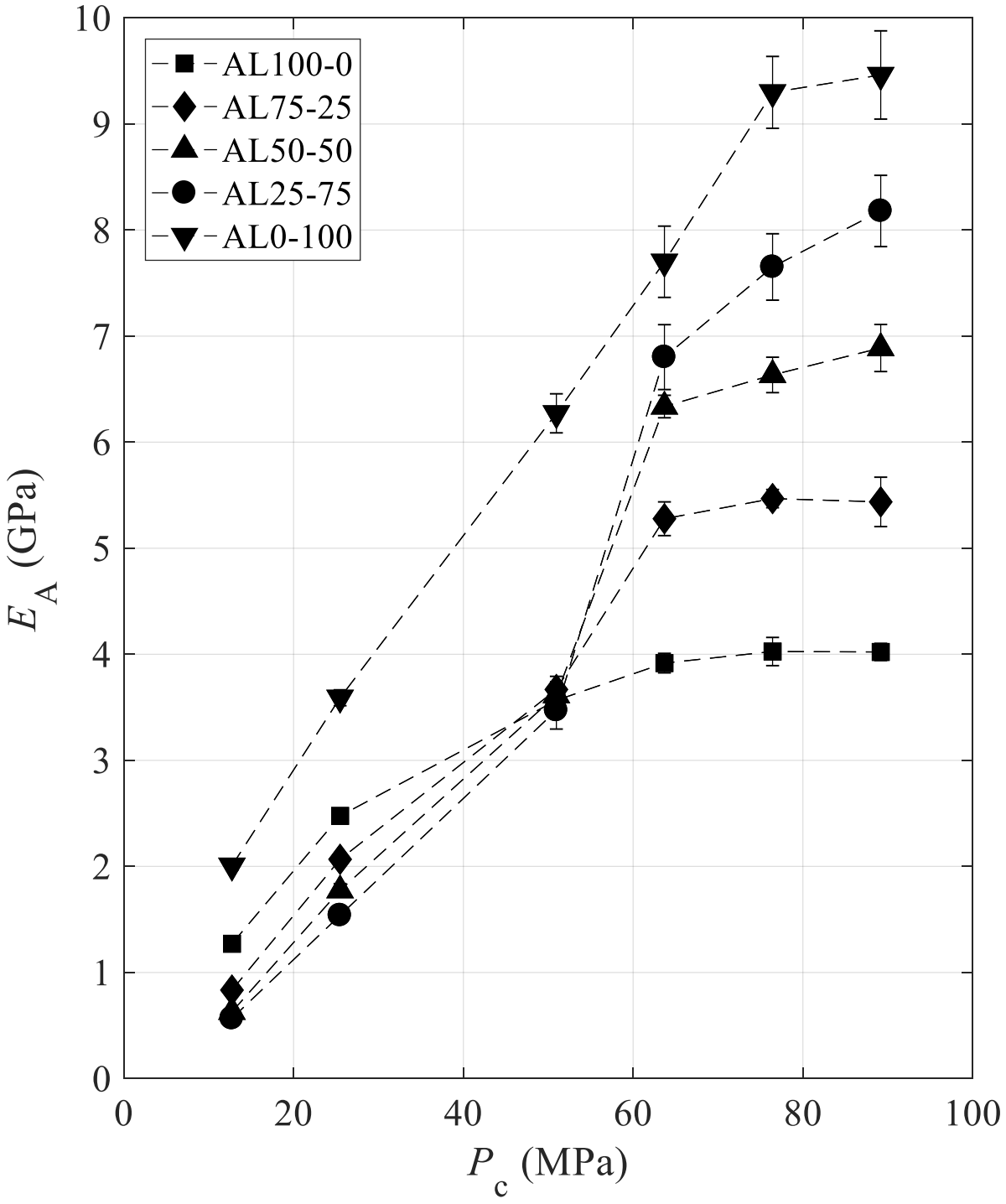
AL100-0
AL75-25
AL50-50
AL25-75
AL0-100
E_A (GPa)
P_c (MPa)
0
1
2
3
4
5
6
7
8
9
10
0
20
40
60
80
100

Figure 2.c

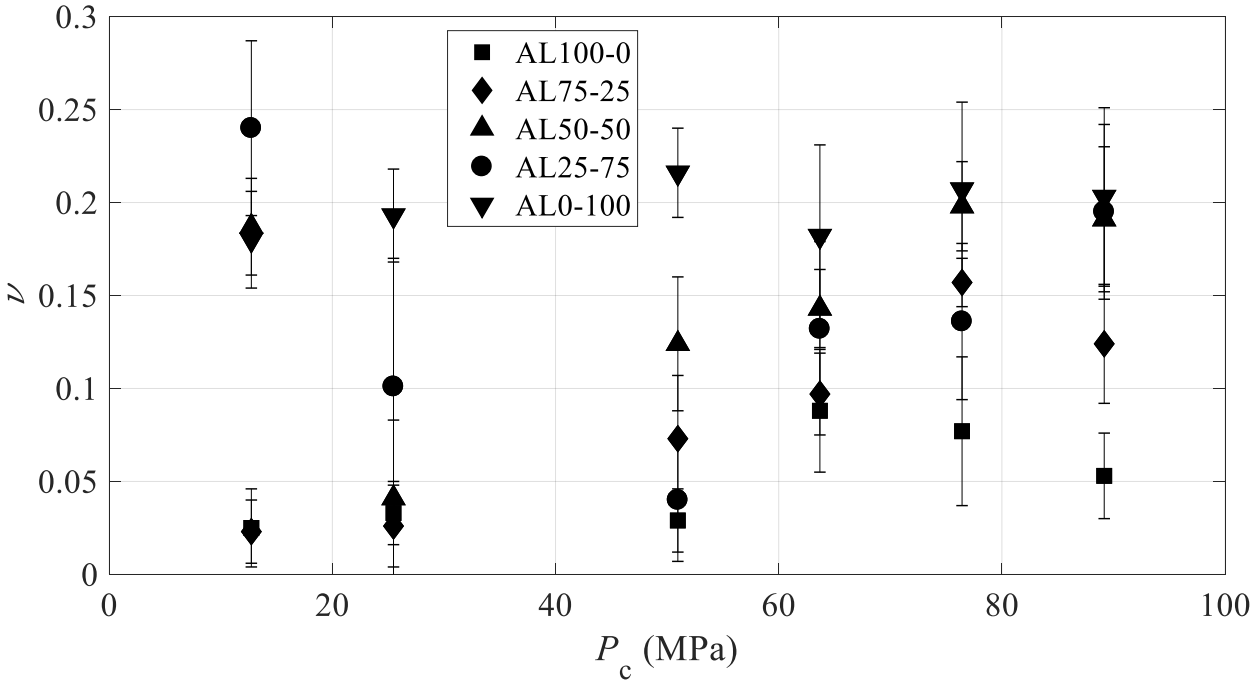

Figure 2.d

Figure 2. Relationship between the compaction pressure (P_c) and the measured material properties: (*a*) pressure (c_L) and (*b*) shear wave speeds (c_T), (*c*) average Young's moduli (E_A), and (*d*) Poisson's ratio (v) of the compact materials acquired using the pitch-catch experimental configuration for the five sample sets.

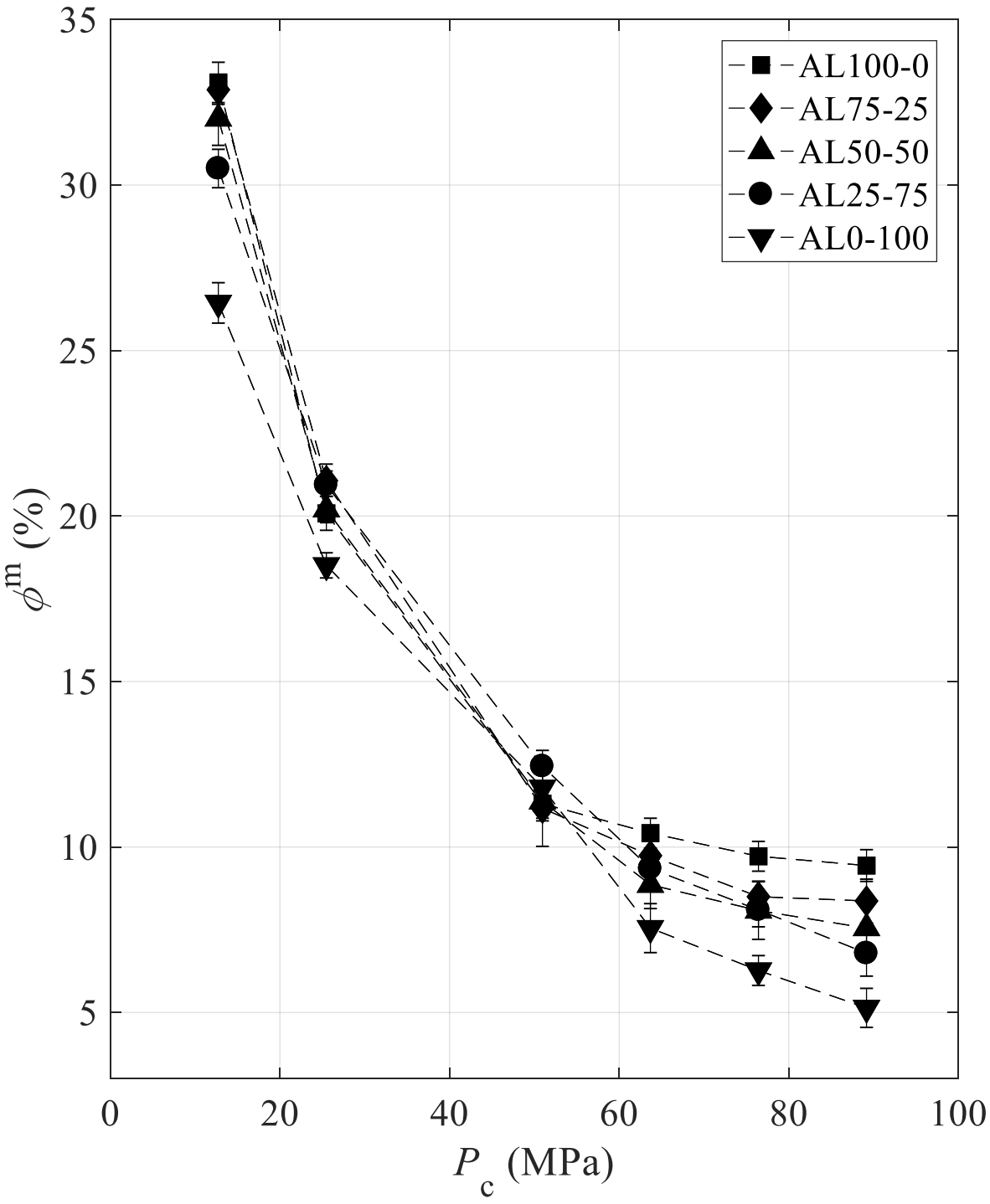
AL100-0
AL75-25
AL50-50
AL25-75
AL0-100
35
30
25
20
15
10
5
0
20
40
60
80
100
ϕ^m (%)
P_c (MPa)

Figure 3.a

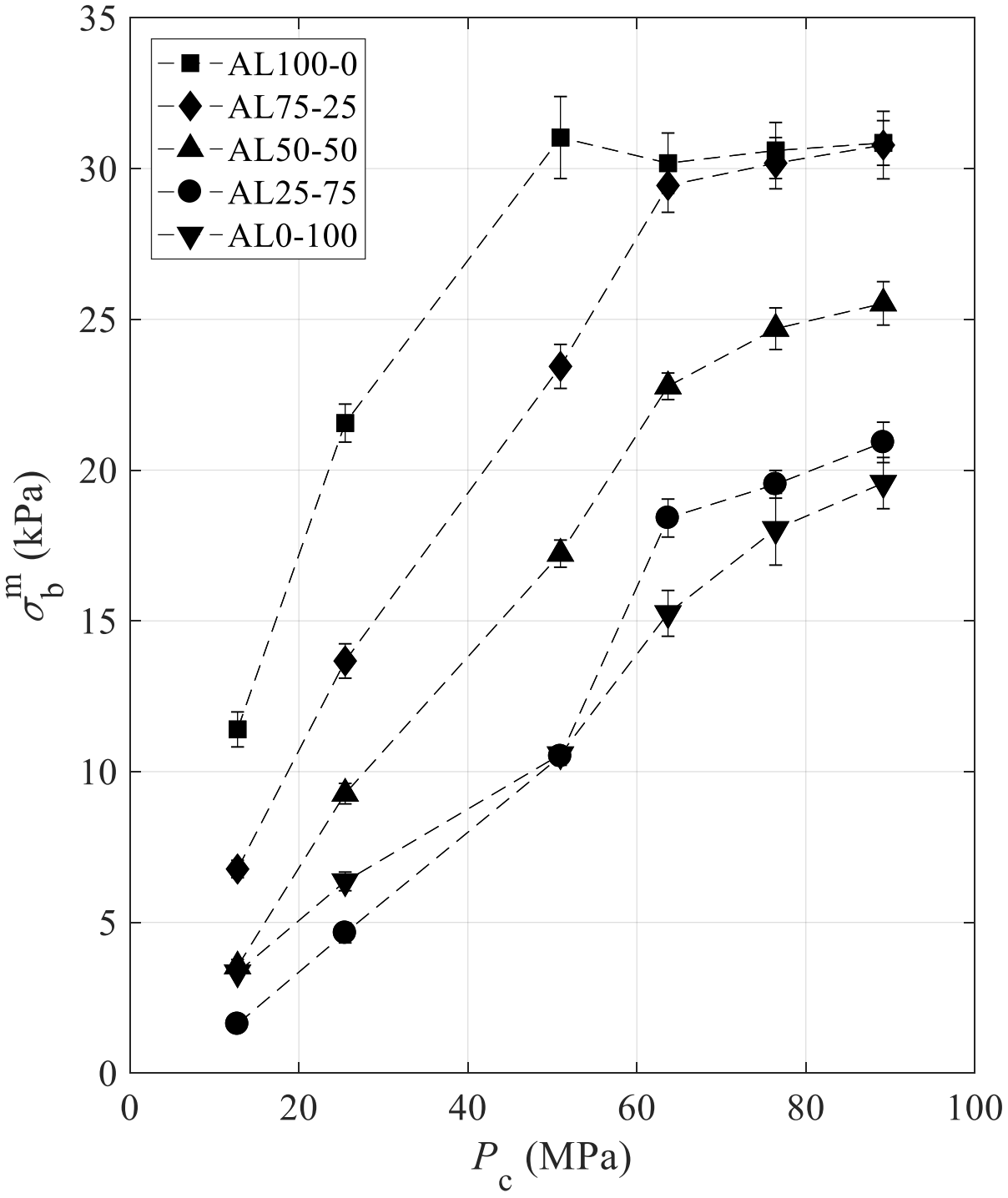
AL100-0
AL75-25
AL50-50
AL25-75
AL0-100
σ_b^m (kPa)
P_c (MPa)
0
5
10
15
20
25
30
35
0
20
40
60
80
100

Figure 3.b

Figure 3. Relationship between the compaction pressure (P_c) and the directly measured properties: (*a*) porosity ratio (ϕ^m) and (*b*) tensile strength (σ_b^m) for the five sample sets.

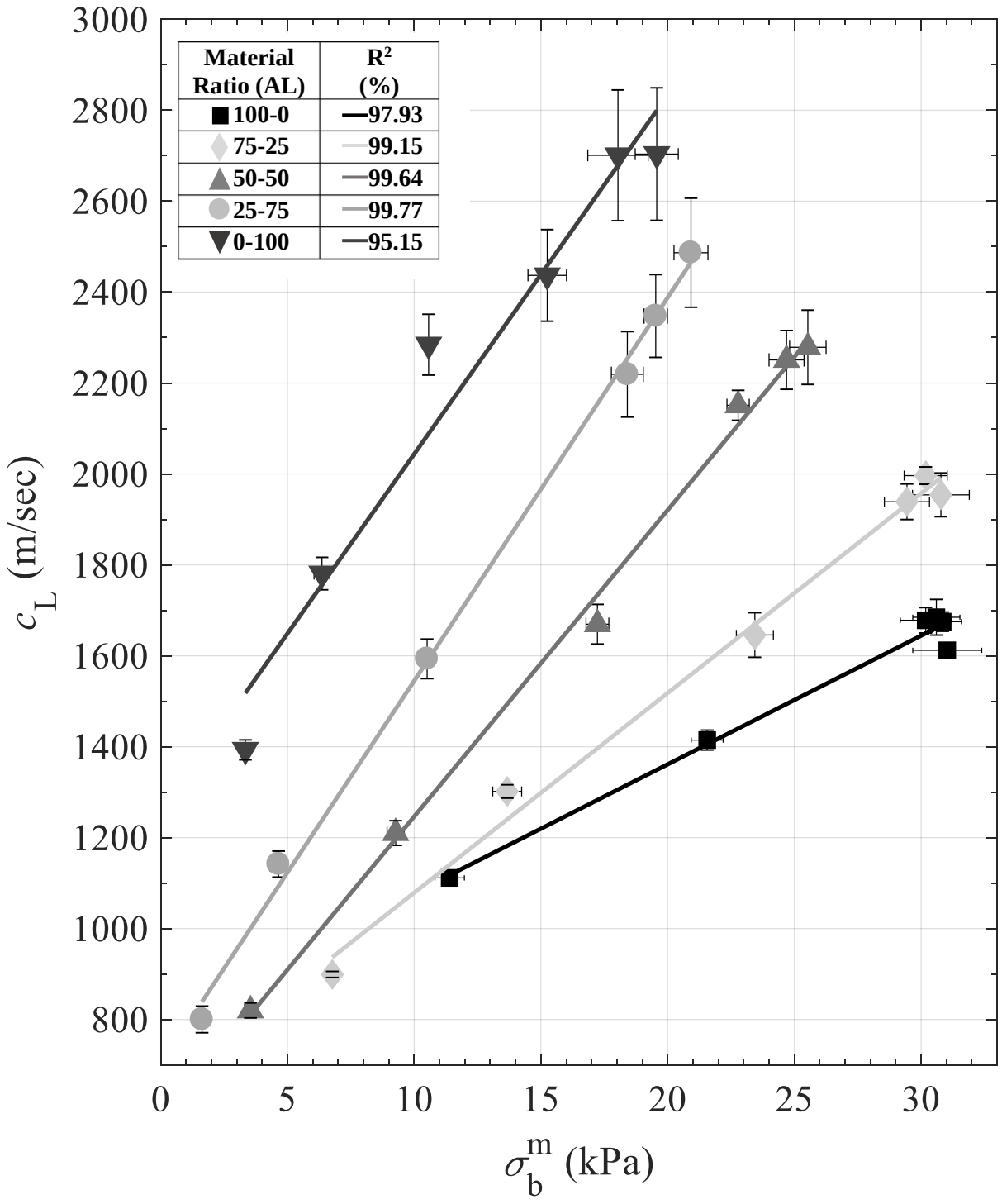
Material Ratio (AL)
R² (%)
100-0
97.93
75-25
99.15
50-50
99.64
25-75
99.77
0-100
95.15
3000
2800
2600
2400
2200
2000
1800
1600
1400
1200
1000
800
0
5
10
15
20
25
30
c_L (m/sec)
σ_b^m (kPa)

Figure 4.a

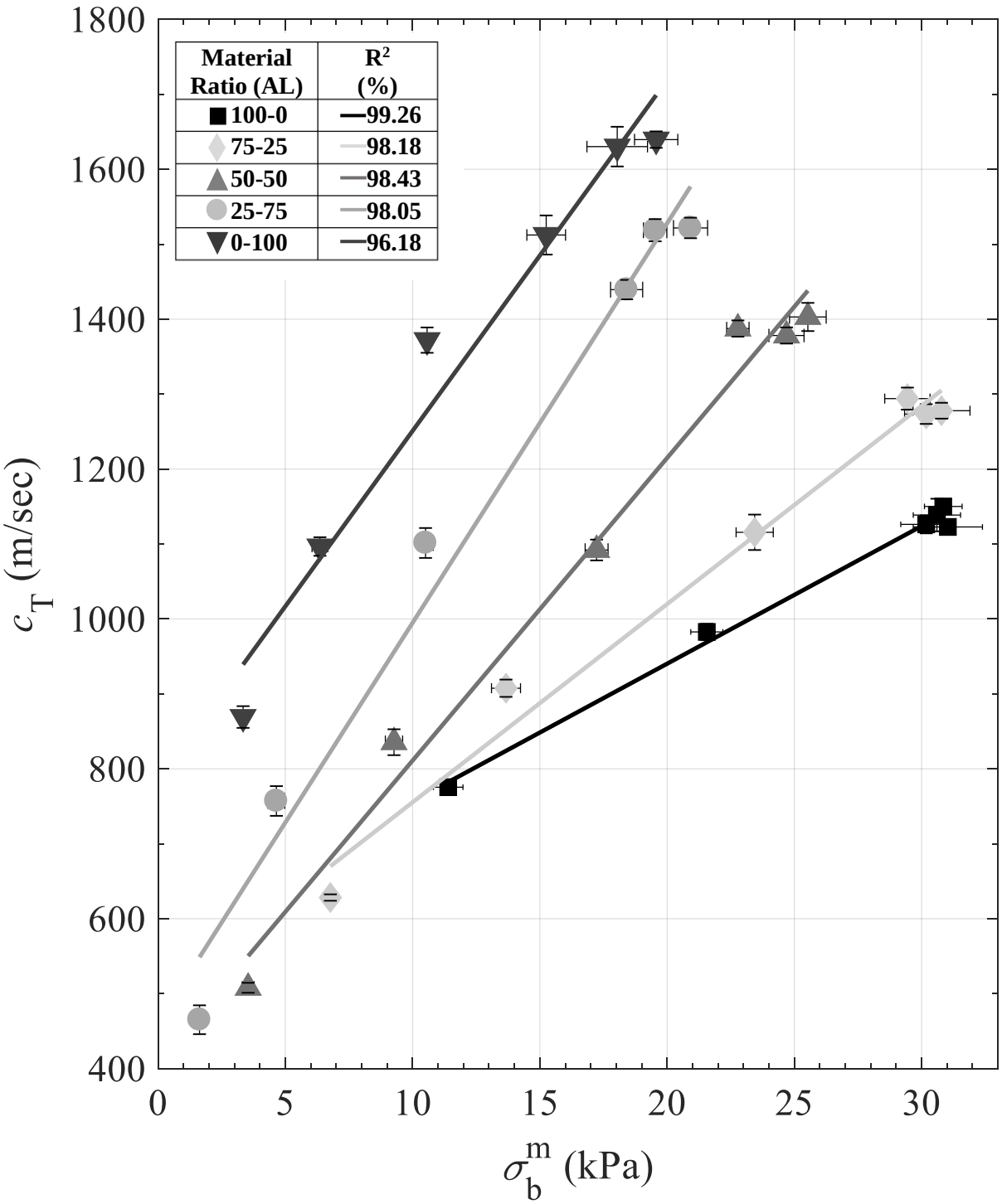
Material Ratio (AL)
R² (%)
100-0
99.26
75-25
98.18
50-50
98.43
25-75
98.05
0-100
96.18
1800
1600
1400
1200
1000
800
600
400
0
5
10
15
20
25
30
c_T (m/sec)
σ_b^m (kPa)

Figure 4.b

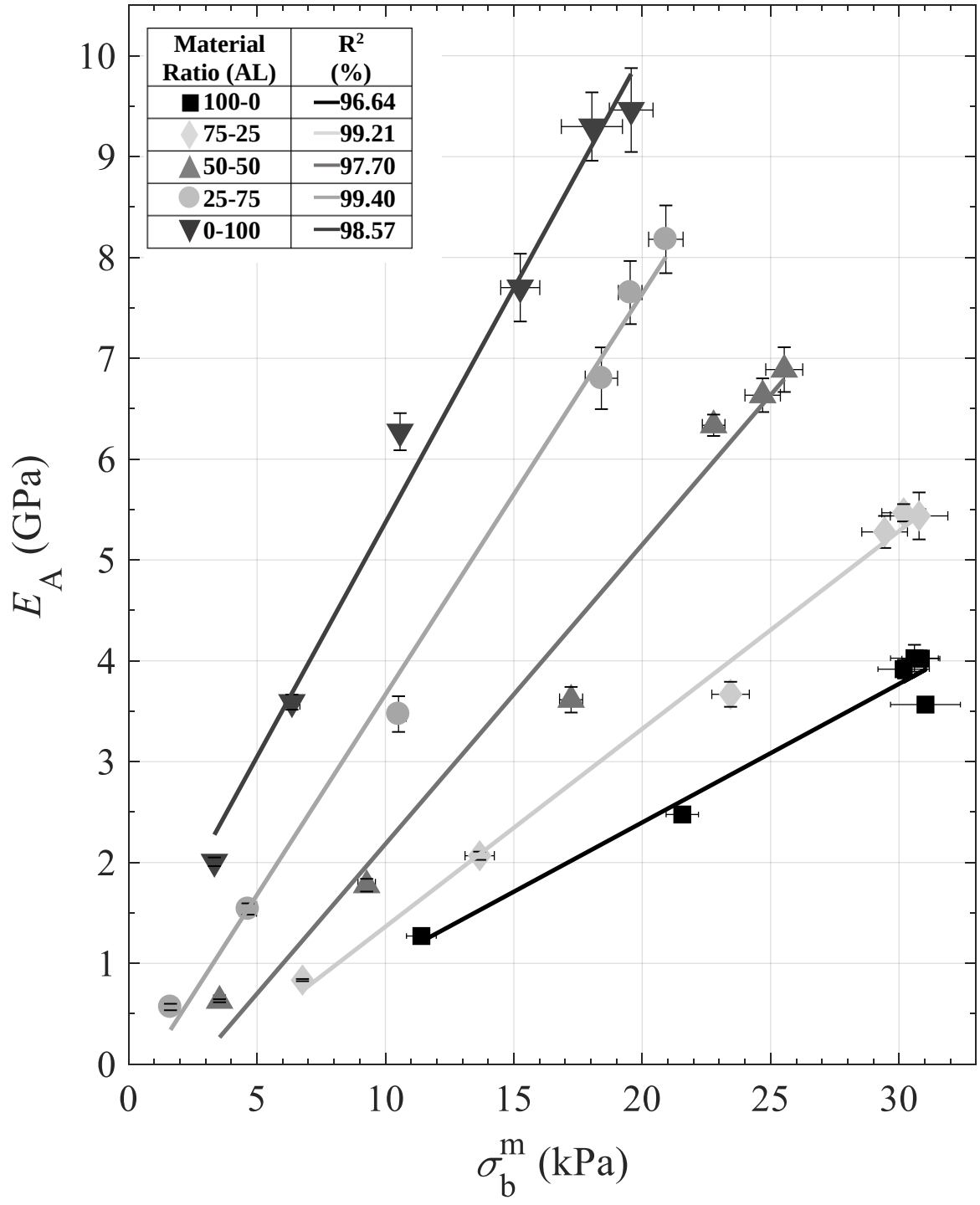
Material Ratio (AL)
R² (%)
100-0
96.64
75-25
99.21
50-50
97.70
25-75
99.40
0-100
98.57
E_A (GPa)
σ_b^m (kPa)
0
1
2
3
4
5
6
7
8
9
10
0
5
10
15
20
25
30

Figure 4.c

Figure 4. Relationships between the directly measured tensile strength (σ_b^m) and acoustically obtained material parameters: (*a*) c_L, (*b*) c_T, and (*c*) E_A (extracted) for the five sample sets with corresponding R^2 (left legend).

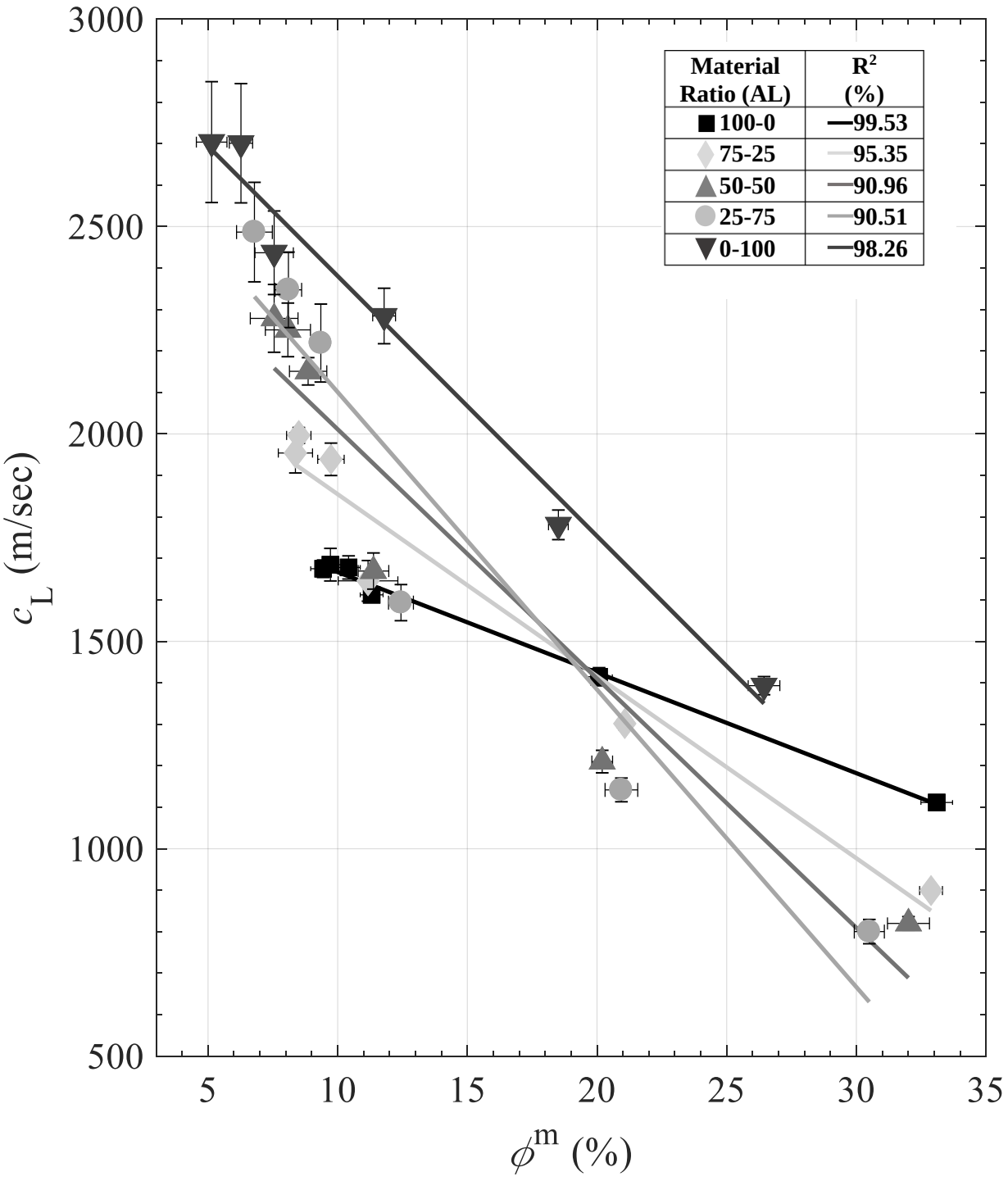
Material Ratio (AL)
R² (%)
100-0
99.53
75-25
95.35
50-50
90.96
25-75
90.51
0-100
98.26
3000
2500
2000
1500
1000
500
5
10
15
20
25
30
35
c_L (m/sec)
ϕ^m (%)

Figure 5.a

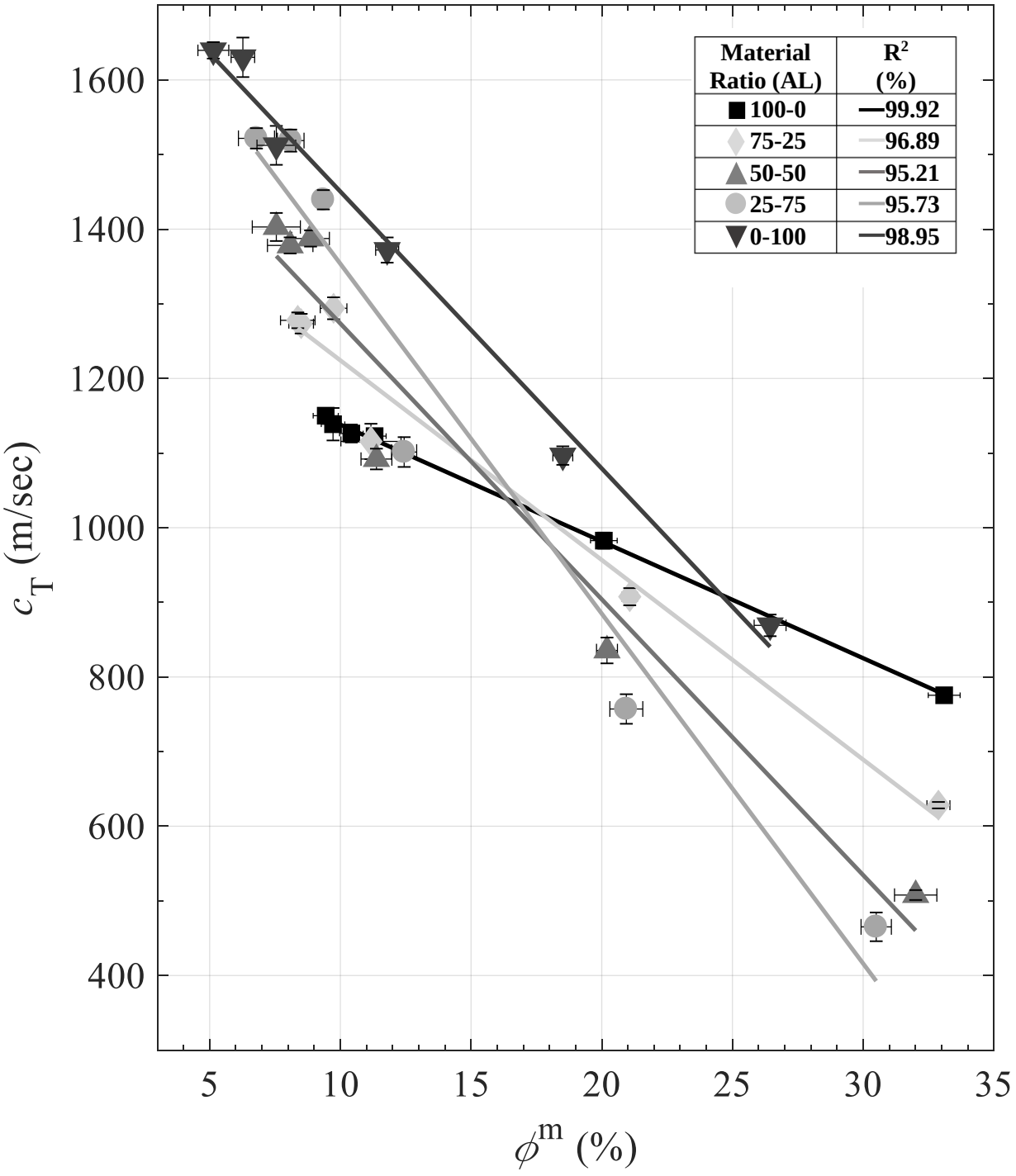
Material Ratio (AL)
R² (%)
100-0
99.92
75-25
96.89
50-50
95.21
25-75
95.73
0-100
98.95
1600
1400
1200
1000
800
600
400
5
10
15
20
25
30
35
c_T (m/sec)
ϕ^m (%)

Figure 5.b

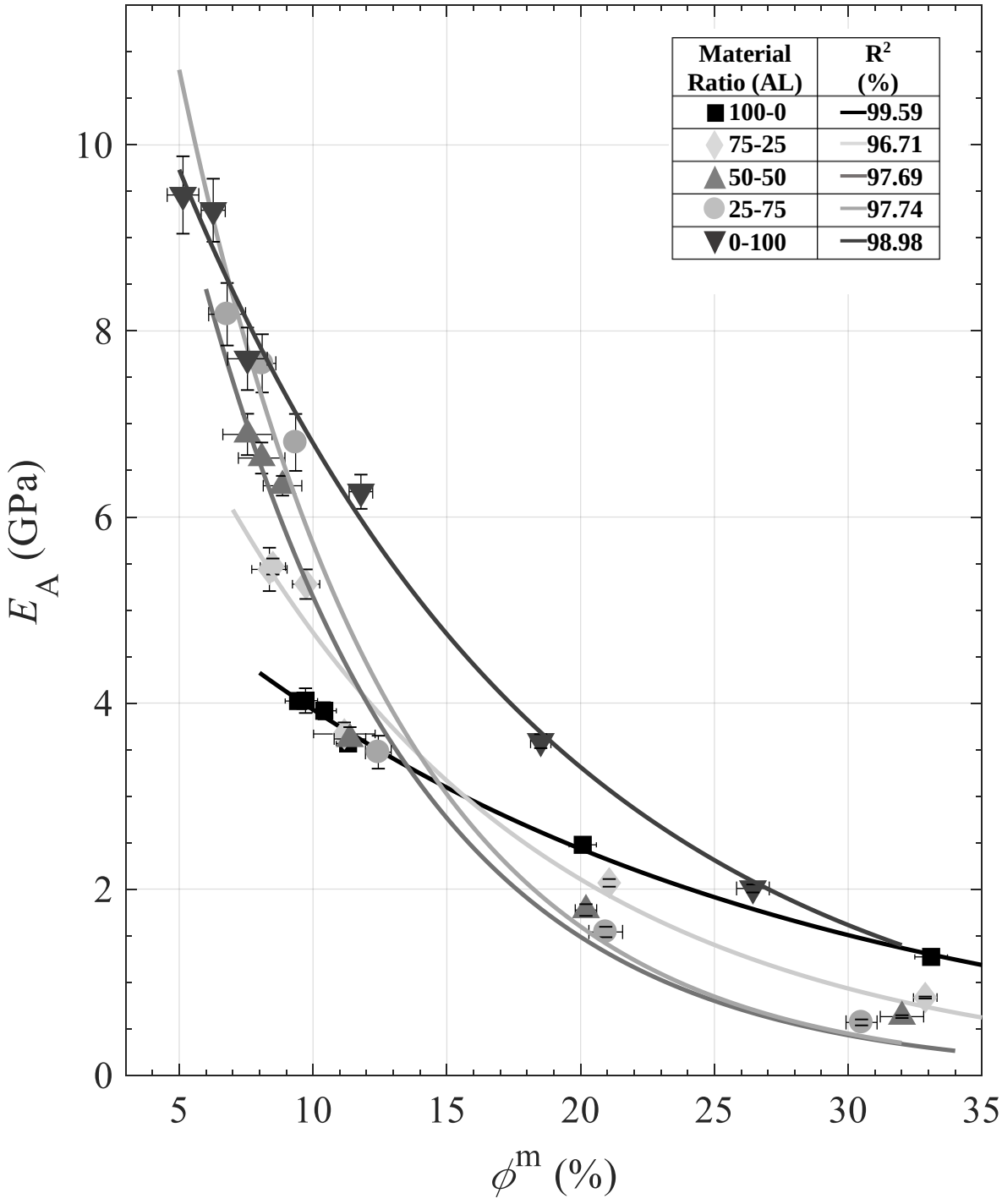
Material Ratio (AL)
R² (%)
100-0
99.59
75-25
96.71
50-50
97.69
25-75
97.74
0-100
98.98
E_A (GPa)
ϕ^m (%)
0
2
4
6
8
10
5
10
15
20
25
30
35

Figure 5.c

Figure 5. Relationships between the directly approximated porosity ratio ϕ^{m} and acoustically determined parameters: (*a*) c_L, (*b*) c_T, and (*c*) E_A (extracted) for the five sample sets with corresponding R^2 values (right legend).